Global and Planetary Change
June 2021, Volume 201, Pages 103498
https://doi.org/10.1016/j.gloplacha.2021.103498
https://archimer.ifremer.fr/doc/00691/80344/

A ~240 ka record of Ice Sheet and Ocean interactions on the Snorri Drift, SW of Iceland

Andrews J.T. [1,*], McCave I.N. [2], Syvitski Jaia [1]

[1] INSTAAR & Dept. Geological Sciences, University of Colorado, Boulder, CO 80309, USA
[2] Godwin Laboratory for Palaeoclimate Research, Department of Earth Sciences, University of Cambridge, Downing Street, Cambridge CB2 3EQ, UK

* Corresponding author : J. T. Andrews, email address : andrewsj@colorado.edu

Abstract :

Core MD99-2323 was extracted from the Snorri Drift at a water depth of 1062 m, just south of the Denmark Strait, and ~120 km from the Last Glacial Maximum (LGM) margins of the Iceland and East Greenland Ice Sheets. The core chronology (~7.5 to 240 cal ka) is derived from radiocarbon dates, marker tephra, paleomagnetic excursion, and correlation with North Atlantic δ18O records on Neogloboquadrina pachyderma (δ18ONp). Sedimentation averaged ~7.5 cm/kyr. Records of proxy flow speed, ice rafted debris (IRD) and oxygen isotopes show that many IRD abundance peaks represent winnowing of the fine fraction by faster flows rather than pulses of increased IRD flux. The overall pattern of flow speed does not resemble the classic fast interglacial/slow glacial pattern seen in records of Nordic Sea overflow, rather the current record is suggested to be partly controlled by the production of brine-driven gravity flows from adjacent ice fronts, especially during cold periods. On a smaller scale the usual glacial/slow – interglacial/fast pattern appears to be the case during ~5 kyr oscillations during Marine Isotope Stage (MIS) 6 where periodic low flow speed is matched by high values of planktonic oxygen isotope ratios. Eight peaks in quartz wt% reflect increased contributions from glacial erosion of Precambrian and Caledonian bedrock from E and NE Greenland; peaks in dolomite may reflect glacial-marine transport from the Laurentide Ice Sheet. Cross wavelet analysis of the δ18ONp versus sortable silt and quartz records indicate significant precession and obliquity periodicities, but with little temporal correlations due to leads and lags in responses.

Highlights

► 240 cal ka record of changes in current speed and grain-size ► Snorri Drift----Northern-most Atlantic sediment drift ► Changes in mineral composition indicate changes in sediment sources. ► Grain-size and mineral records implicate links to orbital forcing. ► MD99-2323 within 130 km of the limits of the Iceland and Greenland ice sheets

Keywords : Snorri Drift, Deep Northern Boundary Current, MIS 1-7, mineral composition, Sortable silt, Flow speed, Saline gravity current, IRD

1.0 Introduction

We explore temporal changes in sediment properties and ocean behavior using data from a ~18 m-long Calypso piston core that was collected from Snorri Drift in 1999 (Labeyrie et al., 2003: Labeyrie & Jennings, 2005) (Fig.1A & B). Snorri Drift lies at the southern end of Denmark Strait, west of Breidavik, Iceland (Egloff and Johnson, 1979; Dunhill, 2005; Parnell-Turner et al., 2015) (Fig. 1). The core was retrieved in 1062 m of water at 65° 25' N, 28° 19' W, somewhat east of the major outflow of Denmark Strait Overflow Water (DSOW) (Dickson & Brown, 1994; McCartney, 1992). The site lies close to the upper limit of the Deep Northern Boundary Current (DNBC), which mainly comprises Iceland-Scotland Overflow Water (ISOW) and at times DSOW (McCartney, 1992). The MD99-2323 (henceforth MD2323) core location lies within ~120 km of the outer limits of the Late Glacial Maximum (LGM) Iceland and Greenland ice sheets (Andrews, 2008; Funder et al., 2004; Patton et al., 2017) (Fig. 1A).

Several factors influence sedimentation and sediment provenance on the Snorri Drift: 1) changes in the proximity of the Iceland and Greenland ice sheets (reflected in grain-size and mineralogy of sediments delivered by iceberg rafting and glacial sediment plumes); 2) changes in the thermohaline-forced DNBC, which contains and interacts with overflow waters (McCartney, 1992); 3) changes in water depth over Snorri Drift resulting from the interplay between glacial isostasy and eustasy, all of which are ultimately controlled by orbital variations in insolation; and 4) July variation in solar insolation at 65°N that is dominated by the precession cycle (Berger and Loutre, 1991).

A variety of paleoclimate data from sites on or adjacent to Snorri Drift (Fig. 1) have been published (e.g. Andrews et al., 1998 [HU93030-007]; Bond and Lotti, 1995 [VM28-14]; Hagen and Hald, 2002 [JM96-1225]; Dunhill, 2005 [MD99-2322]; Andrews et al., 1998 and 2017 [MD99-2260], Voelker, 1999; van Kreveld et al., 2000 [PS2644], McCave and Andrews, 2019b [many cores]). Kuijpers et al. (2003) reported on cores and bottom current activity over the last 20 kyr at sites along the SE Greenland slope (~63.5 °N), and Prins et al. (2002) discussed the competing influences of changes in bottom currents and iceberg rafting on sediments from the Reykjanes Ridge. McCave and Andrews (McCave and Andrews, 2019a, b) assessed flow speeds in the deglaciation and Holocene for many cores in this region including MD2323. Kosters et al. (2004) modelled changes in the DSOW between the LGM and the Holocene. More recently seismic data on Erik Drift, (Muller-Michaelis and Uenzelmann-Neben, 2014) suggests that the strength of the DNBC was reduced during cold intervals and enhanced during warmer periods. Demina et al. (2019) report on geochemical data from core AI-3378 (466 cm long) from 2192 m water depth near the southern limit of the Snorri Drift (59.499° N; -32.842°W), some 660 km from our site and probably affected by sediment transport from the Laurentide Ice Sheets, especially during Hudson Strait Heinrich Events (HS-H) (Jonkers et al., 2010, 2012; Hemming, 2004).

Our paper is based on data initially assembled and analyzed by Dunhill (2005), additional provenance data and analyses extending the record back to an estimated ~243 kyr BP, and quantitative X-ray diffraction (qXRD) estimates of non-clay and clay mineral proportions for the last ~85 kyr in core MD2323. We have compared these findings with similar data from core PS2644 in the Blosseville Basin at the northern end of Denmark Strait (Andrews et al., 2017; Andrews and Vogt, 2020; Andrews and Vogt, 2020).

We investigate for statistically significant associations in core MD2323 between the near-surface record of changing global ice volume and temperature modulated by regional oceanographic changes (e.g. Dansgaard-Oeschger (D-O) events; (van Kreveld et al., 2000), and changes in sediment proxies that are linked to changes in ice sheet extent, sediment provenance and transport, and deep ocean flow. We use a single depth/age model for the core so that any associations between variations in $\delta^{18}O$ of *Neogloboquadrina pachyderma* ($\delta^{18}O_{Np}$) and marine sediment proxies are directly comparable. Signals are investigated that can be linked to changes in deep-water ocean flows over Snorri Drift and to the importation of sediment associated with glacial erosion and transport, either through the presence of very coarse grain-sizes and/or from mineral compositions indicative of derivation from distant source(s).

2.0 Oceanography

In Denmark Strait there are few marine sediment cores that capture the most recent 7 kyr (Elliot et al., 1998; Andrews and Cartee-Schoofield, 2003). The absence of mid and late Holocene sediments on Snorri Drift may be the result of the deglacial-early Holocene resumption of the Denmark Strait Overflow Water (DSOW) supply to the N. Atlantic (Fagel et al., 2004; Hillaire-Marcel et al., 2001), resulting in net sediment removal by higher-speed flows. Previous oceanographic focus for this region has been on the origins and processes associated with the DNBC and DSOW (Behrens et al., 2017; Hansen & Osterhus, 2000; Jonsson and Valdimarsson, 2004; Swift, 1984) and the

development of better-known sediment drifts— Bjorn, Gardar and Erik (McCave and Tucholke, 1986; Bianchi and McCave, 2000; Müller-Michaelis and Uenzelmann-Neben, 2014; Rebesco et al., 2014; Parnell-Turner et al., 2015). Hydrographic transects, taken south (Flaxafloi transect) and north (Latrabjarg transect) of Snorri Drift are part of the VEINS Project (Vertical Exchange in the Northern Seas; (http://www.hafro.is/Sjora/), and WOCE line 24N. Both studies suggest that the Snorri Drift below 1000 m depth is overlain by Atlantic Water (~4.5°C and ~34.95 to 35.00‰ salinity). Mooring DS1 on the Latrabjarg transect has been maintained at 650 m water depth since 1996 (von Appen et al., 2017); long-term bottom flow in the center of Denmark Strait is ~0.2 m s^{-1} (210°) and can exceed 0.47 m s^{-1} during overflow pulses.

During glacial periods, overflow was diminished (Kleiven et al., 2011; Müller-Michaelis and Uenselman-Neben, 2016), but not completely shut off at the LGM (Howe et al., 2016; Keigwin and Swift, 2018). At ~1000 m water depth glacial maximum values of $\delta^{13}C$ of ΣCO_2 are ~+1.5‰ (Curry and Oppo, 2005), characteristic of Glacial North Atlantic Intermediate Water.

There have been several studies on the Holocene extent and variations of icebergs, sea ice, and paleoclimate on the Iceland shelf (Cabedo-Sanz et al., 2016; Jiang et al., 2005; Masse et al., 2008) although under present day conditions, there is no evidence of drifting sea ice and icebergs passing over the site. Historical records note occasional occurrences of sea ice on the SW Iceland shelf (Ogilvie and Jonsdottir, 2000; Ogilvie and Jonsson, 2001), and a recent compilation of reported icebergs sightings noted none on the SW shelf (Andrews et al., 2019). Several studies Andrews et al. (2014) suggested that Holocene variations in the speed of DSOW led to the changes in sand-size provenance in core VM28-14 (Fig. 1) and were not an IRD signal as suggestd by Bond and Lotti (1995).

3.0 Glacial history of East Greenland and Iceland ice sheets during Marine Isotope Stage 2 to 7

Cores collected in the late 1980's and early 1990's from the *Polarstern* (Fig. 1, Table 1) and *RV Bjarni Saemundsson*, *CSS Hudson, Jan Mayen,* and Marion Dufresne on cruises north (Scoresby Sund) and south (Kangerlussuaq) of Denmark Strait provided transect data from within the fjords, along their respective troughs, and (Marienfeld, 1992; Mienert et al., 1992; Syvitski et al., 1996) trough mouth fans (TMF) (Fig. 1). These cruises provided some of the initial data on both present-day processes and MIS 2 and 3 paleoceanography and iceberg rafting. The data from the Scoresby Sund TMF (e.g. PS1730, PS1951, Fig. 1) provided some of the first $\delta^{18}O_{Np}$ and IRD data (Nam et al., 1995; Nam and Stein, 1999; Stein et al., 1993; Stein et al., 1996) for events possibly coeval with the Hudson Strait Heinrich ice stream collapses (MacAyeal, 1993) and meltwater responses in tune with Dansgaard-Oeschger oscillations (Dansgaard et al., 1993). Similar results were latter obtained from the Kangerlussuaq TMF (HU93030-007LCF, same site as MD99-2260, Fig. 1,Table 1)(Andrews et al., 1998).

The record of glaciations on either side of Denmark Strait, for times prior to the LGM, is extremely limited for both the Greenland (Alley et al., 2010; Vasskog et al., 2015) and Iceland ice sheets (Geirsdottir, 2011; Geirsdottir et al., 2007). Inferences about ice sheet extent and advance and retreat phases have usually been made from marine records (Vasskog et al., 2015), which entail several explicit or implicit assumptions about ice sheet/ocean interactions. During MIS5 various models indicate a significant reduced Greenland Ice Sheet (Alley et al., 2009; Vasskog et al., 2015), while marine records from the western Nordic Seas and Baffin Bay indicate "that the ice sheet may have undergone significant growth- and retreat phases…" during MIS5d to MIS3 (Vasskog et al., 2015, p. 51). Evidence also indicates that the Greenland Ice Sheet was more extensive on the SW Greenland Shelf during MIS4 versus the LGM (Seidenkrantz et al., 2019). Whether ice-shelves buttressed Greenland ice streams, especially during MIS3 and MIS2, is an ongoing debate (Boers et al., 2018; Jennings et al., 2018; Petersen et al., 2013) but has implications for the expected sediment grain-size and mineral compositions. At MD99-2260 (Table 1, Fig. 1) on the Kangerlussuaq

Trough Mouth Fan (Dunhill, 2005; Andrews et al., 2017), ice had started to retreat from the shelf break by ca 18 kyr. To the north of Denmark Strait there have been several studies that have used information from marine cores to reconstruct variations in the dynamics of the E and NE Greenland Ice Sheet and to evaluate the synchronicity of iceberg rafted debris (IRD)-events with North Atlantic Heinrich (H-) events (Nam et al., 1995; Stein et al., 1996; van Kreveld et al., 2000). Several IRD events, sourced from NE Greenland (Stein, 2008), are recorded in core MD99-2274 on the North Iceland Shelf (Andrews et al., 2020).

On Iceland, Moles et al. (2019) present evidence for a >400 m thick ice sheet at the time of the NAAZII eruption (~55.4 kyr). For both the East Greenland and Iceland ice sheets there is evidence that the ice sheets reached the shelf break above Denmark Strait during the LGM (Andrews, 2008; Andrews et al., 2017; Dowdeswell et al., 2010; Jennings et al., 2006) with retreat commencing ~19 kyr. Ice streams moved toward the southern end of Denmark Strait from both SW Iceland, along the Flaxafloi trough (Geirsdottir et al., 2007; Patton et al., 2017) and Kangerlussuaq Trough (Dowdeswell et al., 2014), which deposited a large trough mouth fan at the base of the slope (Fig. 1) (Andrews et al., 1998; Stein, 1996).

4.0 Methods and Data

Core 2323 is a 17.6 m long core sampled ~ 8 cm for a total of 226 samples (Dunhill, 2005), using a 4-cc container; the number of clasts in some diamicton intervals necessitated an occasional "unconstrained" sample volume. Weight fragments >2 mm was estimated by sieving at 2-4, 4-8, and 8-16 mm size ranges and expressed as the % of the >2 mm fraction (all data archived with www.Pangaea.de).

Grain size of the <2 mm sediment employed a Malvern Mastersizer S Long Bed instrument. Samples were not decalcified, as the presence of detrital carbonate is an important indicator of sediment provenance in this area (Andrews et al., 2017), and foraminifera do not form a large percentage of the sediment (Dunhill, 2005). The median

weight % of calcite is only 4.2%. Weight %s of sediment > 2 mm was obtained by wet sieving through a series of sieves. The program "Gradistat" (Blott and Pye, 2001) was used to obtain descriptive textural data. Estimates of sortable silt (SS%) and the mean grain-size ($\bar{S}\bar{S}$) of the 63 to 10 μm fractions were computed using published methods (McCave, 1995; McCave & Andrews, 2019a). The percentage of material >250 μm in the laser-analyzed sand and finer fraction is held to be ice rafted and immobile under bottom currents here and is designated as 'IRD250'. We use the running downcore correlation between the sortable silt mean size and percentage (McCave and Andrews 2019a) to determine whether the fine fraction (<63 μm) is current sorted. For core intervals where that correlation falls below 0.5, the segment is likely not current sorted and would not indicate a paleoflow record.

Quantitative mineralogy weight percentages from X-ray diffraction (qXRD) were obtained on sediment reserves used for grain-size analysis using the whole-pattern USGS Rockjock v6 method (Eberl, 2003; Andrews et al., 2017a). Results are expressed as percentages or as g/g of sediment dry weight. The accuracy and precision of this method have been addressed in recent papers (Andrews et al., 2019). The potential provenance of sediment mineral mixtures is identified by use of "SedUnMix" method (Andrews and Eberl, 2012) to estimate contributions from up to six sediment source areas (e.g. Andrews and Vogt, 2020).

***N. pachyderma* $\delta^{18}O_{Np}$ and $\delta^{13}C_{Np}$** Twenty specimens per sample in the ≥ 150 μm fraction were analyzed by the Leibniz- Laboratory for Radiometric Dating and Stable Isotope Research in Kiel, Germany using the fully automated Kiel Carbonate Preparation Device and a Finnigan MAT 251 mass spectrometer. All measurements were calibrated to Pee Dee Belemnite (PDB) (Dunhill, 2005; Appendix 4).

Other Data. Magnetic susceptibility and color reflectance measurements from Labeyrie et al., (2003) and Labeyrie and Jennings (2005). were used in correlation. Cryogenic magnetometer data,

extending down to 1450 cm, reduced by the methods of Mazaud (2005), allowed detection of the Laschamp and Blake events for the age model (Dunhill, 2005).

5. Chronology of MD99-2323.

Our age model builds on previous efforts (Dunhill, 2005; Andrews et al., 2017b) and we note that "All age models are wrong…" (Telford et al, 2003), but are improving (Trachsel & Telford, 2017), an appropriate warning, especially given the vexed and largely unknown answer to the question of appropriate ocean reservoir corrections for sites in this area (Butzin et al., 2005; Skinner et al., 2019; Stern and Lisiecki, 2013; Thornalley et al., 2011). Rarely mentioned is the fact that errors are also associated with layer-counting of ice core records (Boers et al., 2017), and the circularity inherent in matching records (wiggle matching) to improve "goodness of fit"(Blaauw, 2012). Given those provisos, radiocarbon dates, tephrachronology, paleomagnetic excursions, correlations to the global benthic $\delta^{18}O$ stack of Lisiecki and Raymo (2005) and to adjacent core PS2644 contributed to a chronology of core MD99-2323 for the last ~243 kyr (Suppl. Fig. S1, Table S1). The average sedimentation rate (SR) is ~16 cm/ kyr down to -6 m core depth below which there is a drop to <8 cm/ kyr. The value of ~16 cm/k kyr is probably too high due to 'stretching' of the top of the core as shown by Skinner and McCave (2003) for cores taken with the Calypso system on *Marion Dufresne.* The $\delta^{18}O_{Np}$ variations from the well-dated core PS2644, north of Denmark Strait (van Krefeld et al., 2000; Voelker and Haflidason, 2015) and the present core south of Denmark Strait (Fig. 1) indicate rather similar rates of sedimentation; for example North Atlantic Ash Zone II (NAAZ-II) is found at 617 and 607 cm respectively (Andrews et al., 2017b). The $\delta^{18}O_{Np}$ data from other cores immediately south of Denmark Strait (JM96-1225 (Hagen & Hald 2002); HU93030-007 (Andrews et al., 1998); VM28-14 (Bond and Lotti, 1995); AI-3378 (Demina 2019); (Fig. 1, Table 1) have comparable records during MIS1, 2, and 3.

The age control for samples >607 cm, the NAAZ-II tephra, is based on its occurrence in Greenland ice cores dated at 55.4 kyr (Svensson et al. 2008). The Blake (~MIS5d/e, 115 kyr) and

Iceland Basin (~188 ka) excursions (Channell et al., 2020) are possible tie points in the paleomagnetic data. There is a conspicuous paleomagnetic excursion centered ~822 cm and a smaller event at 858 cm that have age estimates in our $\delta^{18}O_{Np}$ depth/age model of 104 and 114 kyr; this is probably the Blake Excursion with an age of 115 ka (Channell et al, 2020). A tie point of 115 kyr at 858 cm is used in the age model. The paleomagnetic record ends at core depth 1450 cm (~185 kyr BP), slightly after (above) the 188 ka Iceland Basin Excursion (Channell et al., 2020) and we observe no excursion. Depths >1450 cm are thus older than 188 kyr. The final depth/age model for MD2323 ultimately depends on how the MD2323 record is tied to the global benthic $\delta^{18}O$ stack (Lisiecki & Raymo, 2005). Although correlation of a planktonic record to a benthic stack is not ideal as the planktonic record contains more temperature and salinity signal than benthic records, most of the features of late glacial climate changes, especially the major MIS transitions are displayed here.

The $\delta^{18}O_{Np}$ data for the near surface polar planktonic foraminifera *N. pachyderma* (Fig. 2A) suggests that MIS 2, 5, 6 and 7 can be identified and dated via correlations between the $\delta^{18}O_{Np}$ record for the MIS6/7 boundary. There is some uncertainty in the links to the MIS7 substages, and Dunhill (2005) and Andrews et al (2017) ended the record at ~225 kyr whereas McCave and Andrews (McCave and Andrews, 2019b) suggested the record extends to ~240 kyr. Using this latter model then the SR for the entire core is ~7.2 cm/ kyr.

Age estimates for the sediment proxies (Table 2) were derived by using linear interpolation between the depth/age points. From this model compositional data were placed on a 1- kyr sampling interval using the integration option in AnalySeries (Paillard et al., 1996). This enables direct quantitative correlations between the variables (Table 2, Supplementary Fig. S2). All variables were slightly under sampled (1.04 and 1.07 samples/ kyr respectively for grain-size and mineral composition averaged).

6.0 Results

The age model is partly based on correlation to orbitally tuned isotope records, and this raises the question of the association between the $\delta^{18}O_{Np}$ record and our sortable silt and sediment mineral data; controls through changes in bottom current flow speeds, changes in the supply of glacially derived sediment.

6.1 *N. pachyderma* oxygen isotope data ($\delta^{18}O_{Np}$).

The $\delta^{18}O_{Np}$ ratios (Fig. 2) reflect global ice volume and near ocean-surface temperature and salinity, but also meltwater volume (Griem et al., 2019) as low values of $\delta^{13}C_{Np}$ and $\delta^{18}O_{Np}$ (Stein et al., 1994, Poore et al., 1999), often superimposed on warming events, at ~16, 60, 125, 210 and 238 kyr (Fig. 2). Although it is at ~1 kyr resolution, the major features of isotope stages are clear. DO cycles in MIS3 are not resolved but millennial oscillations are apparent between ~140 and 185 kyr. The steep and early depletion in $\delta^{18}O_{Np}$ coupled with low $\delta^{13}C_{Np}$ at the base of MIS4 may reflect meltwater influence. The record from MD2323 also has considerable similarity with the $\delta^{18}O_{Np}$ record from PS2644 at the northern intake end of Denmark Strait (Figs. 1, and Fig. S3) (van Kreveld et al., 2000; Voelker, 1999).

6.2 Snorri Drift Grain-size facies

Snorri Drift, sitting under the lee of the Iceland-Greenland Ridge, is the closest drift to the Pleistocene Greenland and Iceland ice sheets (Fig. 1). The sediment in core MD2323 ranges from gravel through gravelly mud, slightly gravelly sandy mud (dominant), to slightly gravelly muddy sand to 'pure' mud (Blott and Pye, 2001) (Fig. 3). The <2 mm size fraction comprises sandy silts with a tail of silty sands and a maximum clay content of 30% (Fig. 3B). The core's size spectra capture the fluctuating influence of iceberg rafting and subsequent deep-current modification. Most samples contain fines plus ice-rafted coarse sand/gravel and thus comprise a mixture of directly deposited and immobile coarse fraction and current deposited fine fraction. The two components are not necessarily genetically related. In order to distinguish current sorted (i.e. contourite) mud

from directly deposited (i.e. IRD) mud, the sorting of the fine fraction has been examined via the correlation between the sortable silt mean and percentage (Fig. S4) (McCave & Andrews, 2019a).

6.3 Sortable silt variations and relationships to IRD and $\delta^{18}O_{Np}$.

6.3.1 IRD. Two measures of IRD amount are employed: the percentage by weight >2mm and the % between 250 and 2000 μm of the < 2mm fraction (Figs. 3 and 4). The linear correlation between the two measures at the individual sample level is not strong (R = 0.2). Nevertheless, the lightly smoothed 1-2-1 weighting data in Figure 4 show close correspondence at all but 3 peaks in down-core abundance, two with high IRD250 and one in MIS5b (~100 kyr) with high %>2mm values. The striking downcore peak at 122-118 kyr (MIS5e) is likely related to an increased residual sand percentage from winnowing when there was negligible coarse IRD input. This 120-kyr peak, going from a background of 5-10% to >40% IRD250, implies removal of over 80% of the fine fraction, and the fact that there is hardly any >2mm material supports the inference that this was not an IRD input event.

6.3.2 Flow speed and IRD. Analysis of the sortable silt mean size ($\overline{SS}$) versus SS% shows a moderately-sorted signature with a correlation coefficient of 0.72 (supplementary Fig. S5A and Figs. 5 & 6 in McCave & Andrews, 2019a). Correlation between $\overline{SS}$ and percentage of medium-very coarse sand >250 μm and gravel >2 mm is weak (r = 0.25, 0.206, respectively); (supplementary Fig. S5 B, C) suggesting that sortable silt mean size is not normally affected by the input of IRD (a few intervals contain high $\overline{SS}$ and high sand values, possibly related to high flow speed winnowing (Figs. 4, 5). The running downcore nine-point correlation coefficients identify a poorly sorted region around 118-122 kyr where the $\overline{SS}$ data might not indicate a flow speed event (Supplementary Fig. S1). Significant portions of the record contain IRD percentages between 15% and 25% but the correlation coefficient between the silt parameters remains greater than 0.75

indicating that IRD and SS are not genetically related in a depositional sense, although they may qualify as a diamicton facies (McCave & Andrews, 2019a).

A pattern of increases in $\overline{SS}$ and IRD250 is seen, especially in MIS7 and 6, but also later in the record (Fig. 5a, b). This association identifies events at the following ages: 202, 188, 164, 152, 140, 120, 110 and 29 kyr. These IRD250 (sand) peaks likely represent winnowing events rather than periods of increased IRD input flux. These five strong pulses of flow in MIS7-MIS6 show no effect of poor sorting of the fine fraction. Some of the IRD peaks are associated with $\delta^{18}O_{Np}$ maxima (colder conditions) (Fig. 6c) in both warm and cold isotope stages.

6.3.3. Flow Speed and Deep Northern Boundary Undercurrent. For core MD2323, the $\overline{SS}$ proxy of minimum flow speeds occurs during MIS7b, during the transition from MIS7a to MIS6, and again at the end of MIS6 into early MIS5e, where $\overline{SS}$ is low but rises to a peak in MIS5e at ~120 kyr. However, the latter peak has a poorly sorted fine fraction from which an inference of flow speed is not warranted (McCave & Andrews 2019a). Nevertheless, this represents the interval where winnowing under a fast flow has removed >80% of the fine fraction. What appears as an anomaly is the predicted higher flow speed during MIS4. There is also a broad increase in flow speed with pulses throughout interglacial MIS5 and a decrease during MIS3. The core's fine fraction during the Holocene interval is not well sorted but the record lacks the core top material (0 - 7.6 kyr).

6.3.4. Flow speed and $\delta^{18}O_{Np}$ sub-orbital oscillations. A striking set of oscillations in the downcore $\delta^{18}O_{Np}$ record are seen in the MIS6 interval (Fig. 6). There is a common association between high $\delta^{18}O_{Np}$ and low flow speeds (Fig. 6 yellow bars), whereas for the MIS3 interval, the relationship is absent (Suppl. Fig. S8). The record also contains associations of high $\delta^{13}C_{Np}$ with high $\delta^{18}O_{Np}$ indicative of meltwater events in MIS3 but less so in MIS6 (Suppl. Figs. S6, S7).

6.4. Sediment mineralogy and provenance

The location of MD2323 (Fig. 1) is such that the main suppliers of glacial sediment would be from the Iceland and Greenland ice sheets, hence we expect that the minerals in core samples would be enriched in a suite of mafic-rich minerals such as pyroxene, plagioclase, and olivine. The qXRD data for MD2323 have been used to define "mineral facies" (Andrews and Vogt, 2020) and the qXRD data are available on www.Pangaea.de (Andrews et al., 2017a). Here we initially focus on four minerals that provide information on broad provenance sources and paleoenvironments---quartz, pyroxene, calcite, and total clay mineral wt%. Felsic-rich sediments with significant amounts of quartz and K-feldspar have to be exported to the Snorri Drift (Fig. 1) either from glacial IRD and sediment plumes from NE Greenland (Andrews and Vogt, 2020) or the Laurentide Ice Sheet, or from bottom currents. Glacial abrasion is such that clay-sized sediments in these areas are dominated by quartz and feldspars (Andrews and Eberl, 2007; Kolla et al., 1979). The increase in felsic minerals during MIS2 and 3 (Fig. 7) probably indicates that glacially derived felsic sediments were transported southward through Denmark Strait from the Precambrian Shield and Caledonian outcrops of granites and metamorphic rocks of NE Greenland or even farther (Verplanck et al., 2009). Calcite can reflect both detrital and *in situ* (e.g. foraminifera, coccoliths) sources, with detrital calcite associated with glacial erosion of carbonate bedrock in NE/N Greenland and erosion of Paleozoic outcrops underlying the Laurentide Ice Sheet (as marked by HS-H events (Hesse, 2016; Andrews and Voelker, 2018). If they co-vary with dolomite then this strongly indicates a detrital origin.

Interpretation of variations in quartz abundance (Fig. 7) is limited by the statistical impact of a closed array (Aitchison, 1986). Quartz and pyroxene abundances, although representing felsic- versus mafic-bedrock end members, are also negatively correlated ($r^2 = 0.33$, n = 234); quartz/pyroxene ratios mimic the same structure as the variation in quartz abundance with peaks at ages of 34, 82, 114, 130, 151, 184, 209, and 230 kyr BP. The median abundance of the clay minerals is 27 % (Fig. 7); representing both weathered clay minerals such as kaolinite and smectite

and those derived from bedrock erosion. These two clay-mineral varieties track each other with a notable lower abundance during MIS5.

We investigated the potential upstream glacial source areas for sediments on the Snorri Drift by using the SedUnMix model (Andrews and Eberl, 2012) and incorporating end-member sediment from the NE Greenland Shelf (PS2623; 74.85°N) (Andrews et al., 2016; Evans et al., 2002; Stein, 2008), the East Greenland Shelf (JM96-1210, -1215; Fig. 1A) (Andrews et al., 2015), and the SW Iceland shelf. Previously, Andrews and Vogt (2014; 2020) demonstrated that the mineral composition of sediments in these three regions were distinctly different. The mineral composition of sediments derived from glacial erosion of the 60,000 km^2 E. Greenland early Tertiary flood basalts (Larsen, 1983) and underlying Archaean and Paleoproterozoic granites and gneisses also includes significant percentages of quartz (Andrews et al., 2015). This source area is flanked by large paleo ice streams (Scoresby Sund and Kangerlussuaq) that extended to the shelf break and are associated with large trough-mouth fans (Dowdeswell et. al., 2014; Stein, 1996; Stein et al., 1996). The NE Greenland source reflects glacial erosion of the NE Greenland Caledonides (Higgins et al., 2008) and the MD2323 data shows a slight but noticeable trend for that source area to increase its contribution, whereas the fraction of sediment from basalt source areas has steadily diminished. The unaccounted for mineral fraction shows no specific trend (Fig. 8). Core MD2323 results indicated a close association (86 ± 7%) with the mineral compositions of these 3 source areas: averaging 18 % from NE Greenland Shelf, 39% from E. Greenland, and 30% from SW Iceland (Fig. 8). The reconstructions indicate that the contributions from NE Greenland show an increase in the importance of this source over the 240 kyr versus a steady decrease with sediments attributed to the Iceland Ice Cap (Fig 8).

7. Discussion

7.1 Wavelet analysis of composition and $\overline{SS}$ in relation to $\delta^{18}O_{Np}$

Cross-wavelet analysis is used to reconstruct the time-series and to recover any common periodicities in the data (Prokoph and El Biali, 2008; Roesch and Schmidbauer, 2018a, b), ((Fig. 9, Suppl. Fig. 9). All three sediment proxies, and the $\delta^{18}O_{Np}$ data, share common significant periodicities of ~45 and 23 ky (Fig. 9B, D, F), with quartz and $\overline{SS}$ also sharing a ~9 ky periodicity; wavelet derived reconstructions capture 59 to 39 % of the variance (Fig.9C and E). This is a similar periodicity to that detected in the records from MD99-2274 (Fig. 1) on the north Iceland shelf (Andrews et al., 2020). The cross-wavelet transform plot (Fig. 9A) only includes the phase sense within the p = > 0.1 zone of confidence, indicating the mean sortable silt leads the variations in quartz within the broad 45, 23, and 16 ky bands. Although the proxy records share common periodicities in the precession and obliquity bands there is little event correlation between them (shaded areas Fig. 9C and E) with an explained variance <1%. For SS% and $\overline{SS}$ in relation to $\delta^{18}O_{Np}$, the record from 150 -10 kyr shows coherency at precession frequencies and obliquity (Supp Fig S9).

7.2 Variations in measures of IRD

MD2323 contains a significant amount of IRD (Figs. 3 and 4), but this does not exclude the possibility that the sediment was reworked by bottom currents (McCave and Andrews, 2019a, b). The profound difference in grain-size between till and proximal glacial marine sediments from sites on the E. Greenland and S.W. Iceland shelves (Andrews and Principato, 2002) compared to MD2323 indicate that sediments in the Snorri Drift are depleted in <10 μm fractions and enhanced in grain-sizes >10 μm.

The differences between the two measures of IRD, %->2mm and %-250 μm (Figure 4) are instructive. A high percentage of what is frequently referred to as IRD (i.e. by grain-size, Andrews, 2000) could arise either by greater input from ice rafting or from removal of a large amount of the sea bottom finer fraction by strong currents. Marked differences are seen at 3 peaks, two with greater IRD250 (120 and 205 kyr) and one in MIS5b (~100 kyr) with high %->2 mm values. In

the cases where there is very low IRD input (low %->2 mm) (120 and 205 kyr) the high sand percentage that corresponds to high flow speeds, could result from winnowing removal of the fine fraction under stronger currents. At 205 ka the flow speed record has three peaks as does the IRD250 record (Fig. 5), giving support to the winnowing hypothesis. The peak in IRD > 2mm abundance at 100 kyr is associated with high flow speeds but without concomitant increases in IRD250, perhaps related to higher IRD input flux.

7.3 Flow speeds related to Northern Boundary Current (DNBC) and saline gravity currents

The Snorri Drift site lies at the northern end of the shallowest location of ISOW flowing north along Reykjanes Ridge prior to its incorporation in the overflow system at Denmark Strait. The record of the $\overline{SS}$ as an indicator of changing flow speed (Fig. 5b) shows weak correspondence to other glacial-interglacial ISOW records shallower than 2000 m in the northern North Atlantic which are characterized by high speeds during interglacials and low speeds during glacials and stadials (e.g. Kleiven et al. 2011). The magnitude of these changes in MD2323 is ~4 μm, equivalent to a flow speed change of at least 5 cm/s (McCave et al., 2017) or about half the glacial to interglacial range shown by Kleiven et al. (2011). The predicted higher flow speed during MIS4 appears as an anomaly. There is a broad increase in flow speed with pulses throughout interglacial MIS5 and a decrease during MIS3. Proxy flow-speed minimum occurs at about 135 kyr, at the top of stage 6/onset of stage 5. However, stage 4 contains the fastest flow speeds where slower speeds would have been expected. It is clear that there is an influence on current flow other than simple climate impacts driving the northern boundary current (DNBC) component of the Atlantic Meridional Overturning Circulation (AMOC).

Sortable silt mean size is not generally affected by the input of IRD in MD2323: $\overline{SS}$ has very low correlation with IRD measures (Suppl Info Figs. 5B, 5C). There are six instances of increases in flow speed with correspondingly elevated IRD250 mainly in MIS7 and 6, and also later in the record (Fig. 5a, b; brown stripes). These IRD250 (coarse sand) peaks represent winnowing

events rather than intervals of increased IRD input flux. Similar pulses, although less obviously connected to IRD %, occurred during MIS5 culminating in the high flow speeds in early MIS4. The range in flow magnitude between the lowest speed in MIS6 and the MIS4 maximum exceeds 10 cm/s.

We suggest that these high-speed pulses mark intervals of downslope saline gravity flows caused by brine rejection during seasonal sea ice formation between the adjacent Greenland and Iceland ice sheets. These would be analogous to the saline outflows in the Weddell and Ross Seas that are the origins of Antarctic Bottom Water (Jacobs, 2004; Gordon et al., 2009; Visbeck & Thurnherr, 2009; Yoon et al., 2020). The core location near the end of the Kangerlussuaq Trough indicates a possible route from a Greenland source for such flows. The flow speed pulses have a magnitude of at least 4 cm/s above the ambient velocity. The record is thus a composite of climatically driven flow with a major overprint from environmentally driven saline gravity currents.

7.4 Millennial oscillations in $\delta^{18}O_{Np}$

A striking set of oscillations observed in the $\delta^{18}O_{Np}$ signal occurs during MIS6 that is correlated with the synthetic Greenland $\delta^{18}O_{ice}$ record constructed by Barker et al (2011). These oscillations are reminiscent of the D-O cycles in MIS3. However, they are paced at ~5-7 kyr as opposed to the dominant 1.5 kyr of MIS3. The record also contains associations of high $\delta^{13}C_{Np}$ (high productivity) with high $\delta^{18}O_{Np}$ (cold) in MIS3 but not in MIS6 (Suppl. Figs. S6, S7). Associated high $\delta^{18}O_{Np}$ and lower flow speeds (buff colour bars, Fig. 6) are attributed to minor meltwater periods where suppressed convection leads to slower bottom water flow.

7.5 Sediment sources

Calcite data (Fig. 7) shows a pronounced peak during MIS5, however, several lesser peaks coincide with low but elevated abundances of dolomite, representing detrital carbonate sources, either from the Paleozoic outcrops of E/NE Canada or N Greenland. Plots of mineral composition for the different source areas (Fig. S10) confirm the importance of these differences. Age estimates for

peaks that rise above background are centered at 24-30, 40-46, 79-85, 87-92, and 131-134 kyr BP. Even with the age uncertainties, and especially the >45 kyr portions of the core, these peaks may indicate correlations with HS H-events noted in cores from the Flemish Cap (Mao et al., 2018). The source(s) for the hematite-stained quartz (HSQ) record from VM28-14 (Fig. 1) (Bond and Lotti, 1995) could be the Devonian sandstone outcrop in NE Greenland and provide a measure of iceberg rafting through Denmark Strait, but given the evidence for winnowing in MD2323 and the lack of correspondence between Holocene E Greenland and Iceland IRD records, HSQ variations may reflect DSOW episodes (Andrews et al., 2014). On the Kangerlussuaq Trough Mouth Fan (core HU93030-007PC, same site as MD99-2260; Fig. 1) (Andrews et al., 1998; Dunhill, 2005), radiogenic ε_{Nd} isotope data from two discrete IRD-rich units suggested a mixed Caledonian and Tertiary basalt source for ice discharge intervals coeval with HS -H) events 2 and -3 (Andrews and Voelker, 2018) and indicates no or limited contribution from the Paleo-Proterozoic bedrock flanking much of the Kangerlussuaq drainage basin.

8. Conclusions

Core MD2323 from the Snorri Drift (Fig. 1) records a complex record of ocean/glacial interactions and sediment responses from 7 to ~243 kyr. We focus on changes in water flow over the Snorri Drift and the importation of sediment to the drift both from the adjacent ice margins and from farther afield. Many parameters are based on samples from the same depth intervals as the $\delta^{18}O_{Np}$ at ~1 kyr spacing, revealing complex associations between $\delta^{18}O_{Np}$ and sediment variables (e.g. Fig. 9). This is also examined in Supplemental material, where we present a non-parametric analysis of the strength of the association between $\delta^{18}O_{Np}$ quartiles and sediment proxies.

Analysis of the sortable silt (10-63 μm) component of the fine fraction demonstrates that most of the core record is well sorted and its mean size provides a valid proxy for palaeoflow speed. The flow speed record shows high velocities during peak interglacials and lower speeds during

glacial maxima as expected on the basis of comparison with other records of the deep boundary currents in the northern North Atlantic. Overall however, the records are not similar. This might be due to over a dozen inferred pulses of flow speed during MIS4, 5a-d and 6, possibly caused by brine from sea-ice formation feeding saline density flows down the East Greenland Kangerlussuaq Trough and off the Iceland Sea ice front, and analogous to contemporary processes in the Ross Sea. Minor meltwater events in MIS6 are likely responsible for millennial reductions in flow speed. Increases in medium to very coarse sand content, often used in analysis of other drift deposits as an index of IRD supply, here frequently correspond to higher flow speeds over the drift and the removal of fines rather than increased IRD delivery.

A sediment unmixing model based on four regional bedrock types indicated considerable changes in the deposition of felsic-rich minerals with two significant pulses during MIS4 and MIS 2 and smaller contributions during MIS6. The most likely source for the felsic minerals (quartz and K-feldspar) would be from glacial erosion by the NE Greenland Ice Sheet, plus potential export from Canadian and Fennoscandian ice-covered Precambrian Shield regions. The continued presence of coarse ice-rafted debris rich in quartz, during the $\delta^{18}O_{Np}$ stadials indicates that there was probably not an ice-shelf across southern Denmark Strait during MIS2 or 6.

Acknowledgements

Our participation in the 1999 IMAGES V cruise was funded by a grant from the National Science Foundation (OPP-0082347 and OCE-98-09001), and two Geological Society of America graduate student grants to Dunhill. Dr. Anne E. Jennings was co-Chief Scientist on this leg of the cruise, along with Dr. Dunhill, and was instrumental in obtaining core MD99-2323 and later supporting the supervision of Dunhill's dissertation. We thank the French captain, crew, and onboard scientists and staff for their help and interest. Gita Dunhill's PhD dissertation, supervised by J. Syvitski, provided the Malvern grain-size data and the stable isotopic data on *N. pachyderma* and contributed to earlier drafts of this manuscript. Some of the analysis presented in this paper are based on a

number of R packages (www. cran.r-project.org/web/packages/) and we are grateful to the various authors of these programs. We thank Simon Crowhurst for the wavelet analysis of $\delta^{18}O_{Nps}$ vs $\overline{SS}$ and SS% in Suppl Fig. 6. We appreciate the comments and criticisms from Drs M. Kirby, A. Voelker, and M.-S. Seidenkrantz on an earlier draft of this paper, and Dr R. Stein and an anonymous referee on the present version.

Conflict of interest

Andrews, McCave, and Syvitski declare that there is no conflict of interest

Table 1: Core locations

Cruise	Station	Long ° W	Lat ° N	Water depth [m]
MD99	2323	-28.34	65.42	1062
MD99	2260	-30.23	63.02	1865
PS2644	2644	-21.7566	67.2683	778
V28	14	29.5667	64.7833	1855
JM96	1225	-29.25	64.91	1683
JM96	1210	-29.6	68.183	452
JM96	1213	-30.9600	67.2883	557
PS	1730	-17.69	70.11	1617
PS	1951	-20.825	68.841	1481
MD99	2274	-17.073	67.582	1000

Table 2

Data	Mag suscept	Color	IRD	Calcite %	18O	13C
sampling cm	2	5	2	8	8	8

orig v 1 kyr	0.67	0.78	0.62	0.83	0.86	0.88
	D(50 µm)	SS%	Ssmean	Clay minerals %	<49	Quartz %
sampling cm	8	8	8	8	8	
orig v 1 kyr	0.87	0.72	0.78	0.74	0.9	0.64

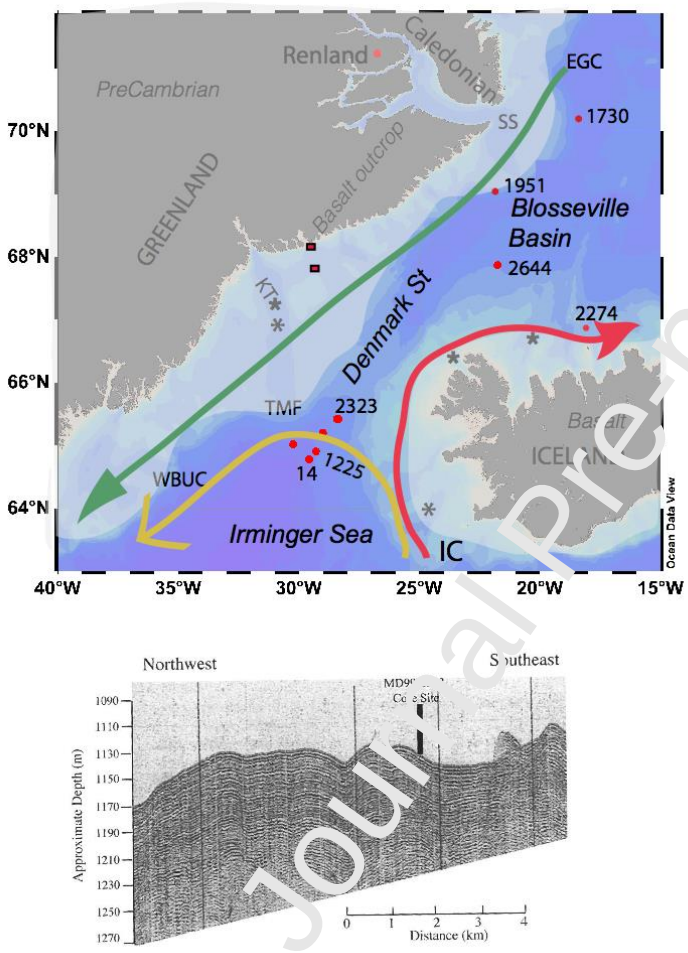

Figure 1: A) Location of core MD99-2323 and other cores noted in the text with LGM limits of the Greenland and Iceland ice sheets schematically portrayed---see Table 1. TMF = Trough Mouth Fan, IC = Irminger Current, WBUC = Western Boundary Undercurrent, EGC = East Greenland Current, KT = Kangerlussuaq Trough (* cores with IRD), filled squares - cores used in the sediment unmixing from East Greenland, SS = Scoresby Sund; B) Seismic profile across the Snorri Drift.

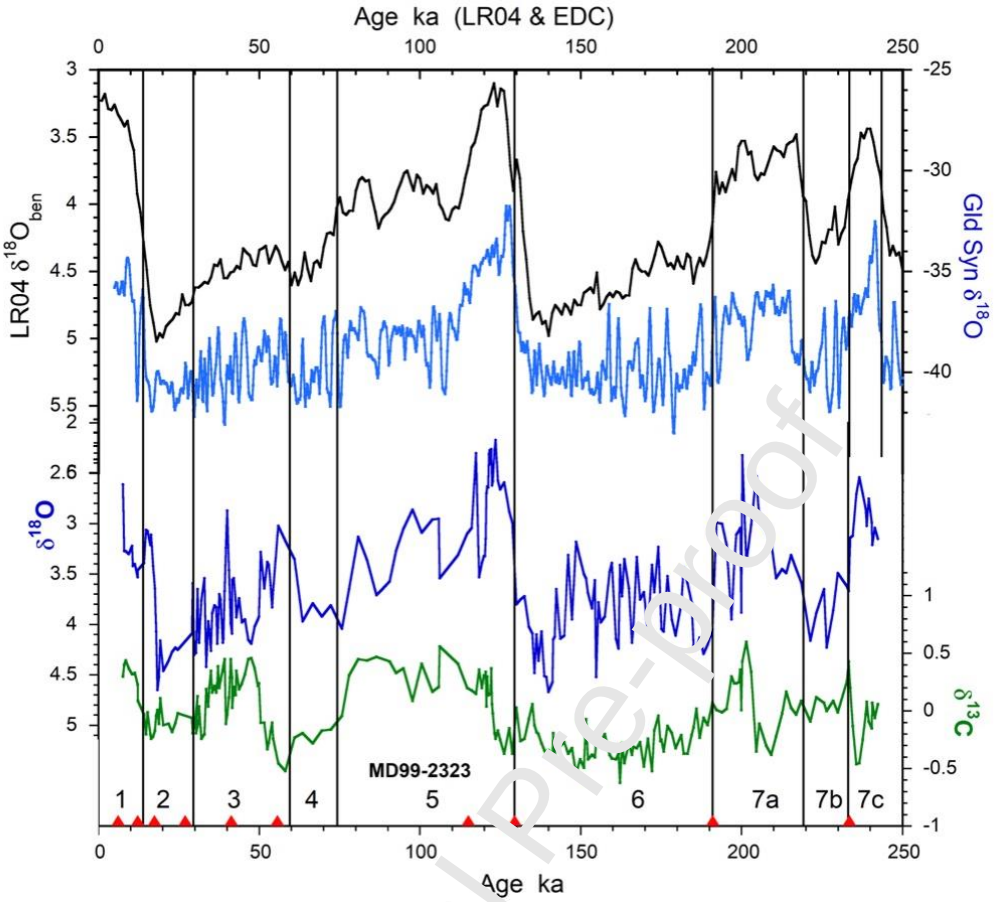

Figure 2. Plot of the subpolar near surface planktonic foraminifera *N. pachyderma* oxygen and carbon isotope ratios $\delta^{18}O_{Np}$, $\delta^{13}C_{Np}$ (Dunhill, 2005) with age. For comparison we have plotted the LR04 benthic $\delta^{18}O$ stack of Lisiecki & Raymo (2005) (black) and the synthetic Greenland $\delta^{18}O_{ice}$ record constructed by Barker et al (2011) based on the thermal bipolar seesaw model relationship between the Antarctic EDC ice core deuterium (D/H) ratio δD and $\delta^{18}O_{ice}$ in Greenland ice cores (GISP2) (blue line) used in construction of the age model. Marine Isotope Stages 1-7 are shown along the bottom. Note low values of $\delta^{13}C_{Np}$ and low corresponding $\delta^{18}O_{Np}$ indicative of meltwater (Stein et al., 1994, Poore et al., 1999) at ~16, 60, 125, 210 and 238 ka.

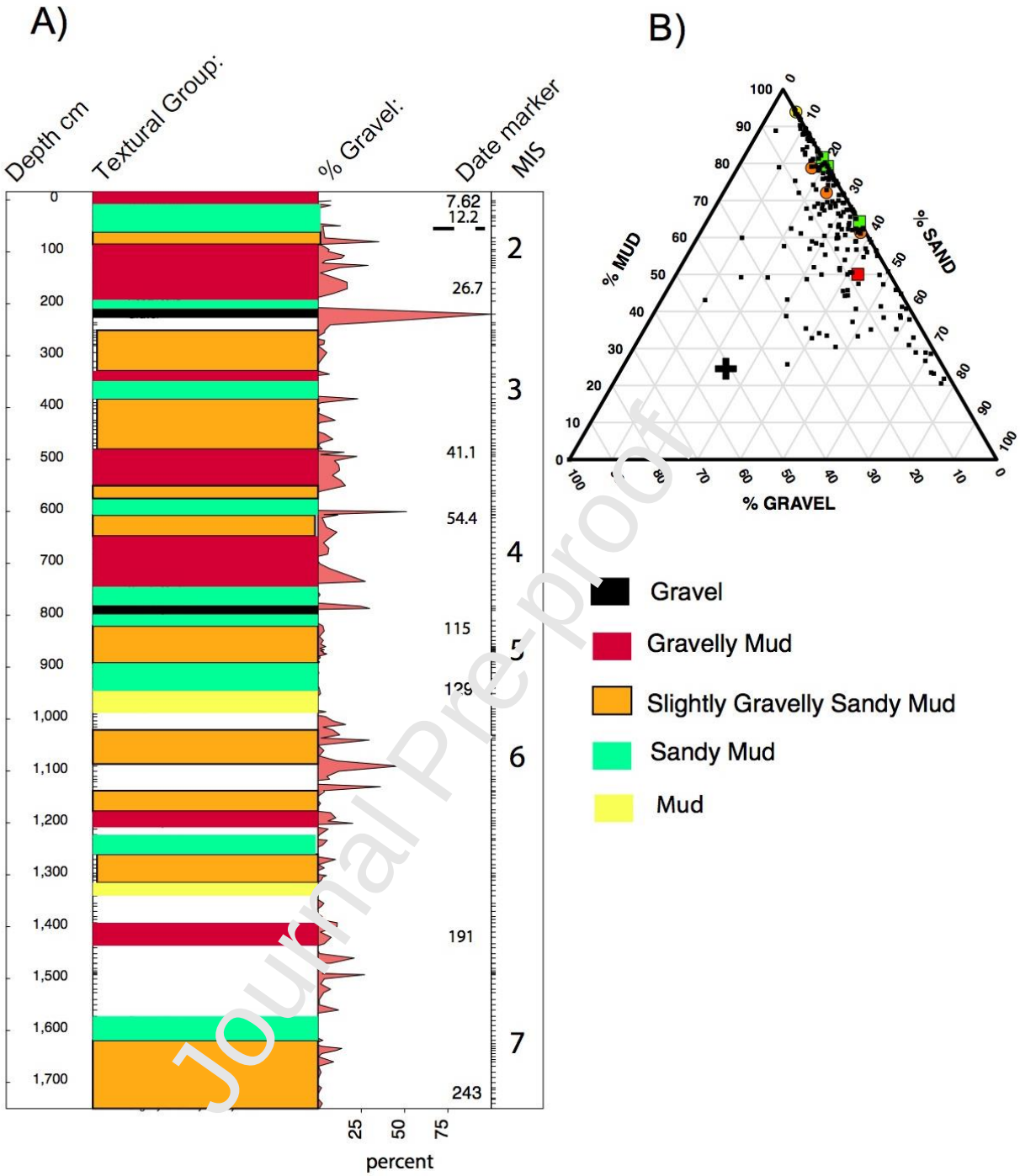

Figure 3: A) Downcore plot of the variations in the textural classification of the MD99-2323 sediment, and the weight % of gravel (> 2mm) in the samples. The location of the age estimates are shown (see also Table S1) and the Marine Isotope Stages B) Gravel, Sand,Mud plot of the sediment samples. Samples representative of the textural classification are plotted with their appropriate color; ther non-colored zones represent either rapid textural changes or rare textures, e.g. gravelly mud.

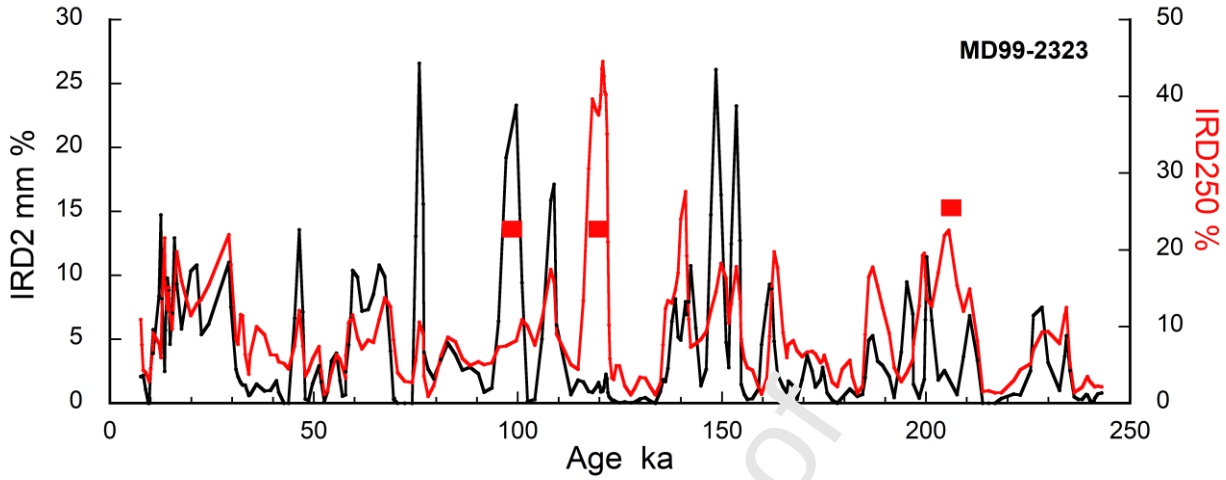

Figure 4. Two measures of ice rafted detritus, % >2mm of the whole sediment (black line) and %>250 μm of the <2 mm fraction (red line), both with a weighted three point smoothing. Red markers indicate the three principal points where there is a large discrepancy between the two measures.

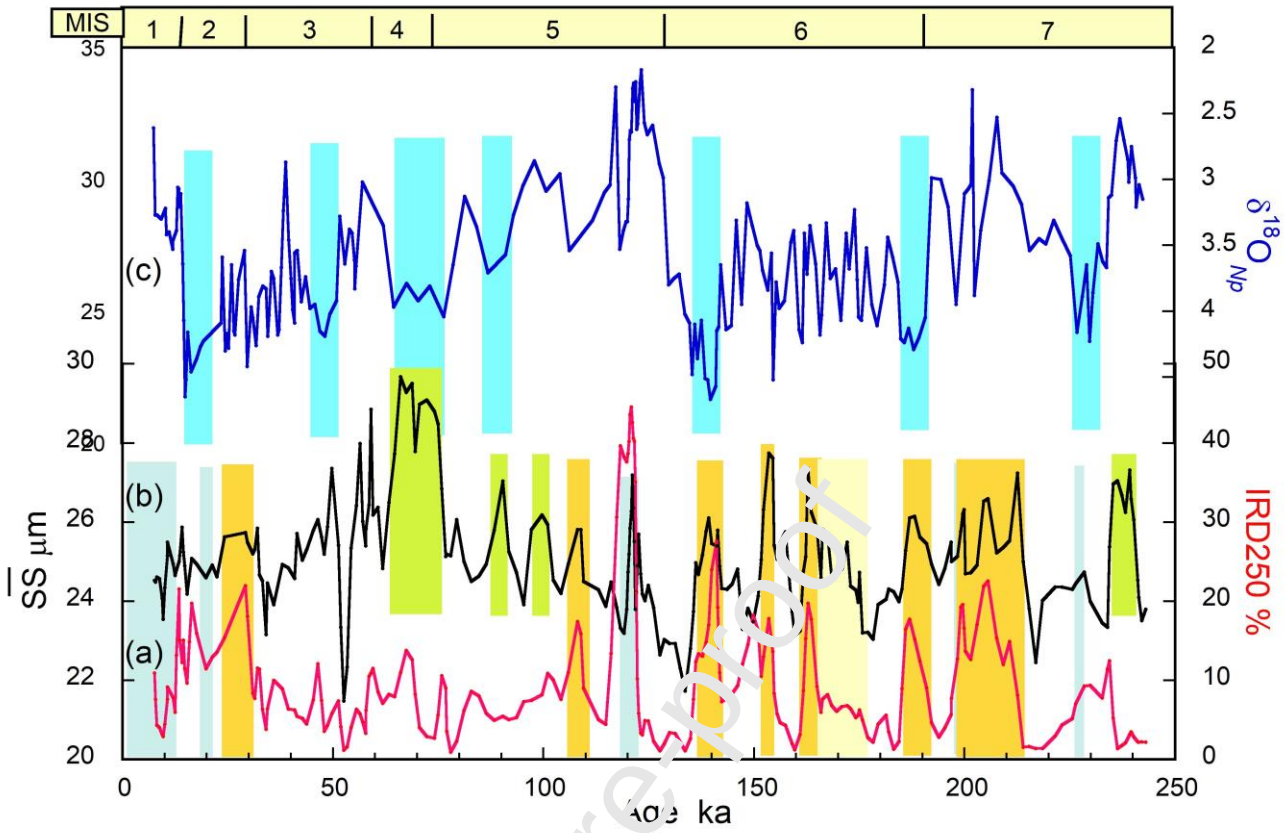

Fig. 5. Sediment and isotopic variables plotted downcore versus age. (a) IRD250%, (b) $\overline{SS}$, (c) $\delta^{18}O_{Np}$. Coloured bars pick out particular features and correspondences between the records: light brown bars (in a & b) mark corresponding peaks of IRD and flow speed, bright blue bars (in c) mark high $\delta^{18}O_{Np}$, likely due to low temperature, some of which correspond to high-speed and IRD, green bars (in b) mark high speed pulses that are not associated with higher IRD, and dull blue bars (in a & b) mark sections of the $\overline{SS}$ record that do not pass the acceptability test of McCave & Andrews (2019a) as a flow speed indicator.

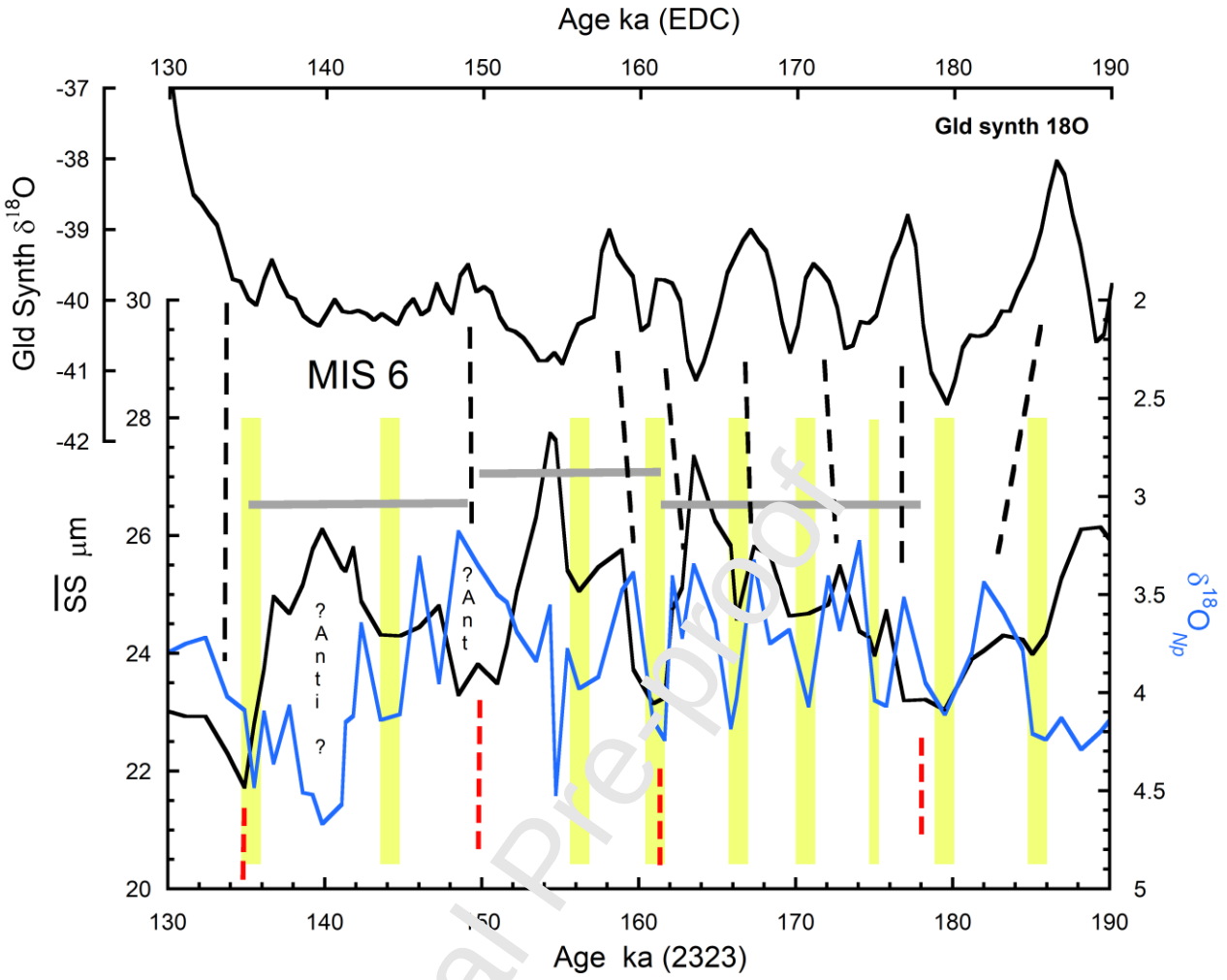

Fig. 6. Sediment and isotopic variability during the MIS 6 oscillations: Sortable silt mean ($\overline{SS}$), $\delta^{18}O_{Np}$, and the synthetic Greenland $\delta^{18}O_{ice}$ record of Barker et al. (2011). Plausible correlations between the isotopic record of $\delta^{18}O_{Np}$ and Greenland are shown by black dashed lines. Red dashed lines mark the high IRD pulses and the grey horizontal bars show the lower speed intervals between them as noted in figure 5. Pale green bars mark the correspondence between low flow speed and high $\delta^{18}O_{Np}$ values suggesting periodically reduced flow during cold events. At two high points this correspondence fails, namely at 140 and 150 ka. The former is the anomaly of high speed at the coldest point of MIS 6 where a downslope saline or cold dense gravity flow is suspected. Perhaps the 150 ka case is similar. See also **Supplementary Figures S3 – S5.**

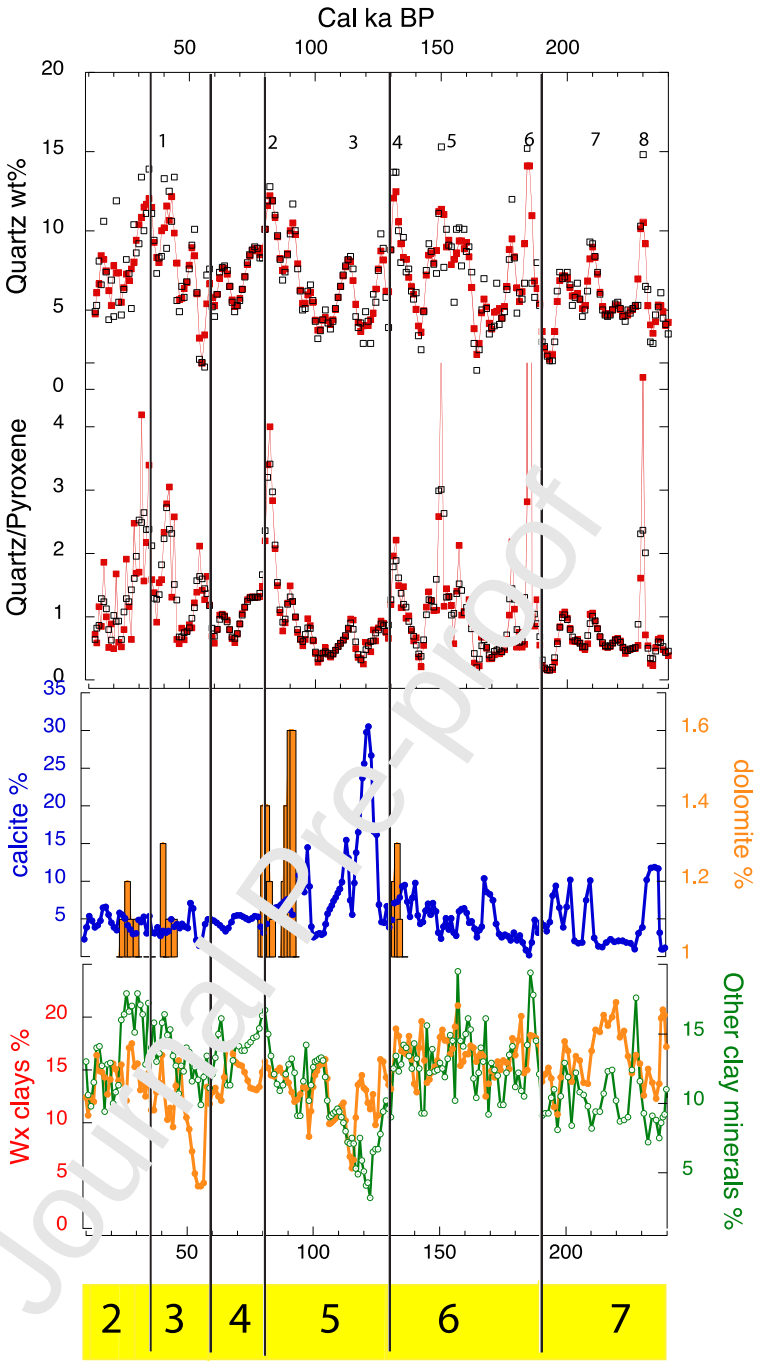

Figure 7: Plots of mineral weight % or ratios based on quantitative XRD. The red lines in the quartz and quartz/pyroxene are 3-point averages. The plot of dolomite (bars) > 1% by weight might indicate transport of detrital carbonate from N Greenland. The weathering (Wx) clays is the sum of kaolinite and smecitite. The vertical black lines demarcate the MIS boundaries.

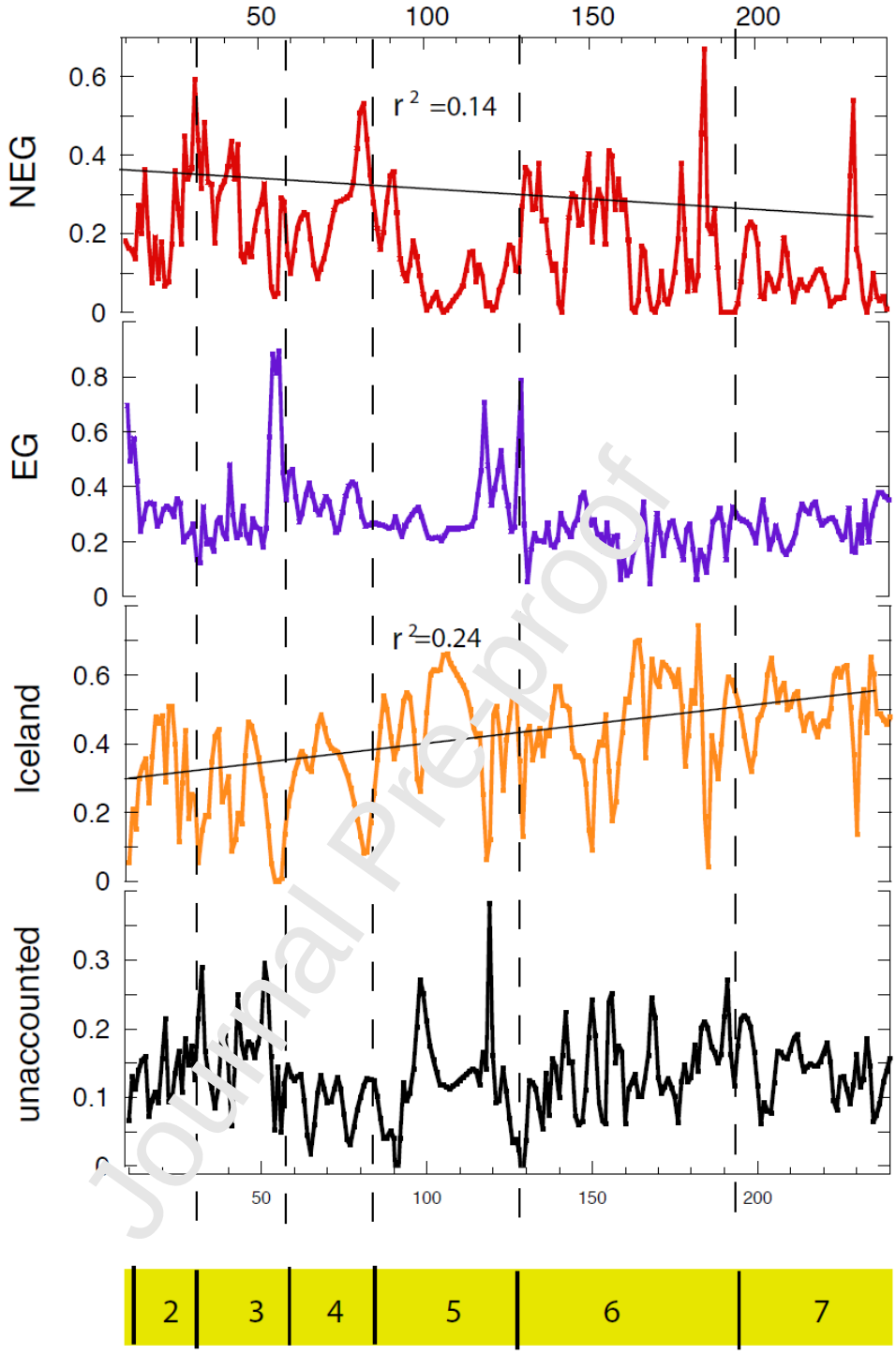

Figure 8: Estimated contribution of sediment to MD99-2323 based on mineral composition from: NEG = NE Greenland (Caledonides), EG = E Greenland, SW Iceland, and the "unaccounted" or residual fraction. The trend lines show the increase or decrease over the last 240 ka BP. The yellow box and black dashed-lines show the Marine Isotope Stage boundaries

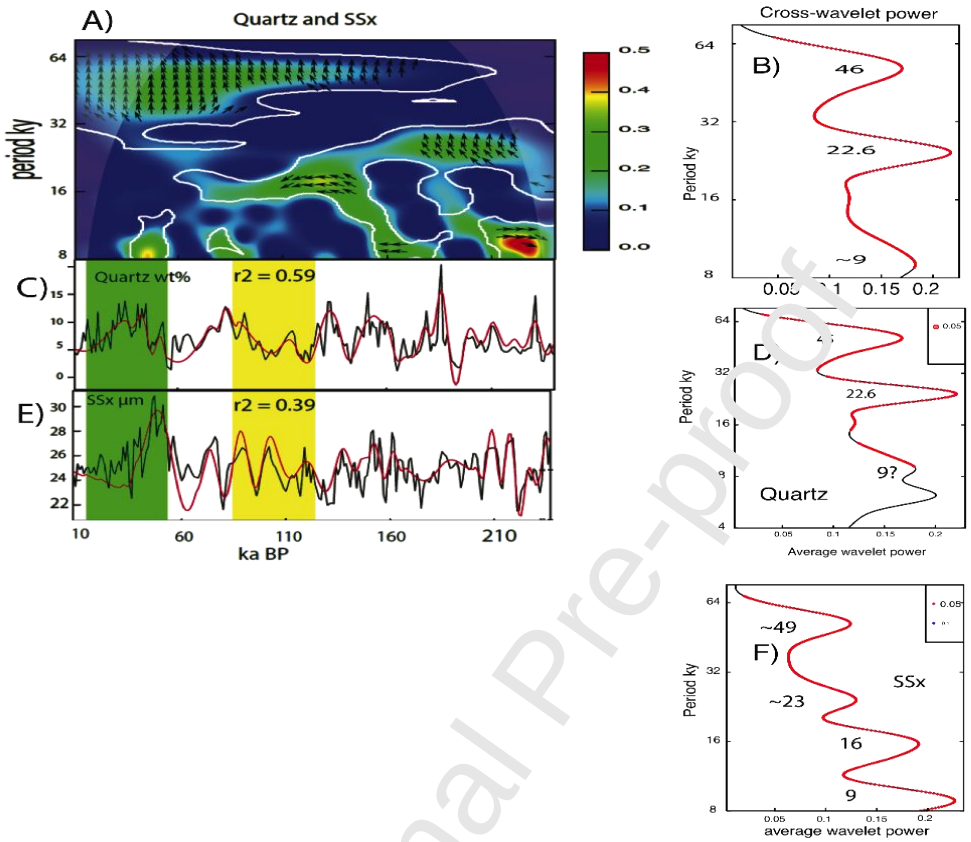

Figure 9: A) Cross-wavelet plot of the variations in quartz wt% and SSx µm in MD2323. This plot shows the 1% confidence area (white line) and the phasing of the two variables within this confidence zone is indicated by the arrows; the cone of confidence is defined by the lightly shaded region. Arrows pointing to the right indicate the records are in phase, to the left out of phase; arrows pointing up mean that SSx leads quartz, and if pointing down then quartz leads SSx. B) cross-wavelet power averaged for quartz and SSx over the 232 ky time slices. C) Variations in quartz (black) and reconstruction (red). D). Wavelet power averaged for quartz. E) Variations in SSx (black) and reconstruction (red). F) Wavelet power averaged for SSx.

References

Alley, R.B., Andrews, J.T., Brigham-Grette, J., Clarke, G.K.C., Cuffey, K.M., Fitzpatrick, J.J., Funder, S., Marshall, S.J., Miller, G.H., Mitrovica, J.X., Muhs, D.R., Otto-Bliesner, B.L., Polyak, L., White, J.W.C., 2010. History of the Greenland Ice Sheet: Paleoclimatic insights. Quaternary Science Reviews 29, 1728-1756.

Andrews, J.T., 2000. Icebergs and Iceberg Rafted Detritus (IRD) in the North Atlantic: Facts and Assumptions. Oceanography 13, 100-108.

Andrews, J.T., 2008. The role of the Iceland Ice Sheet in sediment delivery to the North Atlantic during the late Quaternary: how important was it? Evidence from the area of Denmark Strait. Journal of Quaternary Science 23, 3-20.

Andrews, J.T., 2011. Unravelling sediment transport along glaciated margins (the Northwestern Nordic Seas) using quantitative X-ray diffraction of bulk (< 2 mm) sediment, in: Bhuiyan, A.F. (Ed.), Sediment Transport. InTech, pp. 225-248.

Andrews, J.T., Bigg, G.R., Wilton, D.J., 2014. Holocene sediment transport from the glaciated margin of East/Northeast Greenland (67-80°N) to the N Iceland shelves: Detecting and modeling changing sediment sources. Quaternary Science Reviews 91, 204-217.

Andrews, J.T., Bjork. A.A., Eberl, D.D., Jennings, A.E., Verplanck, E.P., 2015. Significant differences in late Quaternary bedrock erosion and transportation: East versus West Greenland ~ 70°N and the evolution of glacial landscapes. Journal of Quaternary Science 30, 452-463.

Andrews, J.T., Cartee-Schoofield, S., 2003. Late Quaternary lithofacies, provenance, and depositional environments (~12 to 30 cal ka), north and south of the Denmark Strait. Marine Geology 199, 65-82.

Andrews, J.T., Cooper, T.A., Jennings, A.E., Stein, A.B., Erlenkeuser, H., 1998. Late Quaternary iceberg-rafted detritus events on the Denmark Strait/Southeast Greenland continental slope (~65° N): Related to North Atlantic Heinrich Events? Marine Geology 149, 211-228.

Andrews, J.T., Dunhill, G., Vogt, C., Voelker, A.H.L., (2017a): Bulk mineral assemblage with X-ray diffraction of sediment core MD99-2323. PANGAEA, doi:10.1594/PANGAEA.876068,

Andrews, J.T., Dunhill, G., Vogt, C., Voelker, A.H.L., 2017b. Denmark Strait during the Late Glacial Maximum and Marine Isotope Stage 3: Sediment sources and transport processes. Marine Geology 390, 181-198.

Andrews, J.T., Eberl, D.D., 2007. Quantitative mineralogy of surface sediments on the Iceland shelf, and application to down-core studies of Holocene ice-rafted sediments. Journal of Sedimentary Research 77, 469-479.

Andrews, J.T., Eberl, D.D., 2012. Determination of sediment provenance by unmixing the mineralogy of source-area sediments: The "SedUnMix" program. Marine Geology 291, 24-33.

Andrews, J.T., Jónsdóttir, I., Geirsdóttir, A., 2019. Tracking Holocene drift-ice limits on the NW/SW Iceland shelf: comparing proxy data with observation and historical evidence. Arctic, Antarctic, and Alpine Research.

Andrews, J.T., Principato, S.M., 2002. Grain-size characteristics and provenance of ice-proximal glacial marine sediments (or why do grain-size analyses anyway?), in: Dowdeswell, J.A., O'Cofaigh, C. (Eds.), Glacier-influenced Sedimentation at High-Latitude Continental Margins. Geological Society of London, pp. 305-324.

Andrews, J.T., Smik, L., Belt, S., Sicre, M.A., McCave, I.N., 2020. Ocean surface and bottom water conditions, iceberg drift and sediment transport on the North Iceland margin during MIS 3 and 2 Quaternary Science Reviews 252.

Andrews, J.T., Stein, R., Moros, M., Perner, K., 2016. Late Quaternary changes in sediment composition on the NE Greenland margin (~ 73 degrees N) with a focus on the fjords and shelf. Boreas 45, 381-397.

Andrews, J.T., Vogt, C., 2014. Source to Sink: Statistical identification of regional variations in the mineralogy of surface sediments in the western Nordic Seas (58°N – 75°N; 10° W -- 40°W). Marine Geology 357, 151-162.

Andrews, J.T., Vogt, C., 2020. Variations in felsic- versus mafic-sources in the Western Nordic Seas during MIS 1 to MIS 4. Marine Geology 424, Article Number: 106164.

Andrews, J.T., Voelker, A., 2018. "Heinrich events" (& sediments): A history of terminology and recommendations for future usage. Quaternary Science Reviews 187, 31-40.

Barker, S., Knorr, G., Edwards, R.L., Parrenin, F., Putnam, A.E., Skinner, L.C., Wolff, E., Ziegler, M., 2011. 800,000 years of abrupt climate variability, Science, 334, 347-351.

Behrens, E., Våge, K., Harden, B., Biastoch, A., Boning, C.W., 2017. Composition and variability of the Denmark Strait Overflow Water in a high-resolution numerical model hindcast simulation, J. Geophys. Res.Oceans,122, 2830–2846, doi:10.1002/2016JC012158.

Behrens, E.W., 1978. Further comparisons of grain size distributions determined by electronic particle counting and pipette techniques. Journal of Sedimentary Petrology 48, 1213-1218.

Berger, A., Loutre, M.F., 1991. Insolation values of the climate of the last 10 Million years. Quaternary Science Reviews 10, 297-318.

Bianchi, G. G., McCave, I. N., 2000. Hydrography and sedimentation under the deep western boundary current on Bjorn and Gardar Drifts, Iceland Basin, Marine Geology, 165, 137-169.

Blaauw, M., 2012. Out of tune: the dangers of aligning proxy archives. Quaternary Science Reviews 36, 38-49.

Blott, S.J., Pye, K., 2001. GRADISTAT: A grain size distribution and statistics package for the analysis of unconsolidated sediments. Earth Surface Processes and Landforms 26, 1237-1248.

Boers, N., Goswami, B., Ghil, M., 2017. A complete representation of uncertainties in layer-counted paleoclimate archives. Climate of the Past. 13, 1169–1180.

Bond, G.C., Lotti, R., 1995. Iceberg discharges into the North Atlantic on millennial time scales during the last glaciation. Science 267, 1005-1009.

Burgess, P.M., 2016. Identifying ideal stratigraphic cycles using a quantitative optimization method. Geology 44, 443-446.

Butzin M., Prange M., Lohmann G., 2005. Radiocarbon simulations for the glacial ocean: the effects of wind stress, Southern Ocean sea ice and Heinrich events. Earth and Planetary Science Letters 235, 45– 61.

Cabedo-Sanz, P., Belt, S.T., Jennings, A.E., Andrews, J.T., Geirsdottir, A., 2016. Variability in drift ice export from the Arctic Ocean to the North Icelandic Shelf over the last 8000 years: A multi-proxy evaluation. Quaternary Science Reviews 146, 99-115.

Channell, J.E.T., Singer B.S., Jicha, B.R., 2020. Timing of Quaternary geomagnetic reversals and excursions in volcanic and sedimentary archives. Quaternary Science Reviews. 228, 106114, 29pp. doi:10.1016/j.quascirev.2019.106114

Costa, K. M., and 34 others, 2020. ^{230}Th normalization: New insights on an essential tool for quantifying sedimentary fluxes in the modern and Quaternary ocean. Paleoceanography and Paleoclimatology, 35, 2019PA003820.

Curray, J.R., 1961. Tracing sediment masses by grainsize modes, 21st International Geological Congress, Cophenhagen, pp. 119-130.

Curry, W. B., Oppo, D.W., 2005. Glacial water mass geometry and the distribution of $\delta^{13}C$ of ΣCO_2 in the western Atlantic Ocean, Paleoceanography, 20, PA1017, doi:10.1029/2004PA001021.

Dansgaard, W., Johnsen, S.J., Clausen, H.B., Dahl-Jensen, D., Gundestrup, N.S., Hammer, C.U., Hvidberg, C.S., Steffensen, J.P., Sveinbjorndottir, A.E., Jouzel, J., Bond, G., 1993. Evidence for general insatbility of past climate from a 250-kyr ice-core record. Nature 364, 218-220.

Davis, J.C., 1986. Statistics and data analysis in Geology. John Wiley & Sons, New York.

Demina, L.L., Novichkova, E.A., Lisitzin, A.P., Kozina, N.V., 2019. Geochemical signatures of paleoclimate changes in the sediment cores from the Gloria and Snorri Drifts (Northwest Atlantic) over the Holocene-mid Pleistocene. Geosciences, 9, 432. doi:10.3390/geosciences9100432

Dickson, R. R., Brown, J., 1994. The production of North Atlantic Deep Water - sources, rates and pathways. Journal of Geophysical Research-Oceans, 99, 12319-12341.

Dowdeswell, J.A., Evans, J., Cofaigh, C.O., 2010. Submarine landforms and shallow acoustic stratigraphy of a 400 km-long fjord-shelf-slope transect, Kangerlussuaq margin, East Greenland. Quaternary Science Reviews 29, 3359-3369.

Dowdeswell, J.A., Hogan, K.A., Cofaigh, C.O., Fugelli, E.M.G., Evans, J., Noormets, R., 2014. Late Quaternary ice flow in a West Greenland fjord and cross-shelf trough system: submarine landforms from Rink Isbrae to Uummannaq shelf and slope. Quaternary Science Reviews 92, 292-309.

Dowdeswell, J.A., Ottesen, D., Bellec, V.K., 2020. The changing extent of marine-terminating glaciers and ice caps in northeastern Svalbard since the 'Little Ice Age' from marine-geophysical records Holocene 30, 389-40.1

Dunhill, G., 2005. Iceland and Greenland margins: A comparison of depositional processes under differnt glaciological and oceanographic settings. Ph.D. Thesis, Geological Sciences, University of Colorado, Boulder, p. 242.

Eberl, D.D., 2003. User guide to RockJock: A program for determining quantitative mineralogy from X-ray diffraction data. United States Geological Survey, Open File Report 03-78, 40 pp, Washington, DC.

Egloff, J., Johnson, G.L., 1979. Erosional and depositional structures of the southwest Iceland insular margin: thirteen geophysical profiles, in: Watkins, J.S., Montadert, L., Dickerson, P.W. (Eds.), Geological and Geophysical Investigations of Continental Margins. AAPG, Tulsa, OK, pp. 43-63.

Ellenberg, J., 2014. How not to be wrong. Penguin Books, London.

Elliot, M., Labeyrie, L., Bond, G., Cortijo, E., Turon, J-L. Tisserat,N., Duplessy J-C., 1998. Millennial-scale iceberg discharges in the Irminger Basin during the last glacial period. Relationship with the Heinrich events and environmental settings. Paleoceanography, 13, 433-446.

Evans, J., Dowdeswell, J.A., Grobe, H., Niessen, F., Stein, R., Hubberten, H.-W., Whittington, R.J., 2002. Late Quaternary sedimentation in Kejser Joseph Fjord and the continental margin of East Greenland, in: Dowdeswell, J.A., O'Cofaigh (Eds.), Glacier-influenced sedimentation on High-Latitude conintental margins. Geological Society, London, pp. 149-179.

Fagel, N., Hillaire-Marcel, C., Humblet, M., Brasseur, R., Weis, D., Stevenson, R., 2004. Nd and Pb isotope signatures of the clay-size fraction of Labrador Sea sediments during the Holocene: Implications for the inception of the modern deep circulation pattern. Paleoceanography 19, Article Number: PA3002.

Farmer, G.L., Barber, D.C., Andrews, J.T., 2003. Provenance of Late Quaternary ice-proximal sediments in the North Atlantic: Nd, Sr and Pd isotopic evidence. Earth and Planetary Science Letters 209, 227-243.

Folk, R.L., 1954. The distinction between grain size and mineral composition in sedimentary rocks. Journal of Geology 62, 344-359.

Funder, S., Jennings, A.E., Kelly, M.J., 2004. Middle and late Quaternary glacial limits in Greenland, in: Ehlers, J., Gibbard, P.L. and Hughes, P.D. (Eds.), Quaternary Glaciations-Extent and Chronology, Part II. Elsevier, Amsterdam, pp. 425-430.

Funder, S., Kjeldsen, K.K., Kjaer, K.H., O Cofaigh, C., 2011. The Greenland Ice Sheet during the past 300,000 years: A review. In, Ehlers, J., Gibbard, P.L. and Hughes, P.D. (Eds.), Quaternary Glaciations-Extent and Chronology, Part II. Elsevier, Amsterdam, 699-713.

Geirsdottir, A., 2011. Pliocene and Pleistocene Glaciations of Iceland: A brief overview of the Glacial History, in: Ehlers, J., Gibbard, P.L. and Hughes, P.D. (Eds.), Quaternary Glaciations-Extent and Chronology, Part II. Elsevier, Amsterdam, pp. 199-210.

Geirsdottir, A., Miller, G.H., Andrews, J.T., 2007. Glaciation, erosion, and landscape evoloution of Iceland. Journal of Geodynamics 43, 170-186.

Ghil, M., Allen, M.R., Dettinger, M.D., Ide, K., Kondrashov, D., Mann, M.E., Roberston, A.W., Saunders, A., Tian, Y., Varadi, F., Yiou, P., 2002. Advanced spectral methods for climatic time series. Reviews of Geophysics 40, 3-1 to 3-41 1003, doi:1029/2000RG000092.

Griem, L., Voelker, A. H. L., Berben, S.M. P., Dokken, T. M., Jansen, E., 2019. Insolation and glacial meltwater influence on sea-ice and circulation variability in the northeastern Labrador Sea during the last Glacial period. Paleoceanography and Paleoclimatology, 34, 1689–1709. doi:10.1029/2019PA003605

Gordon, A. L., Orsi, A. H., Muench, R., Huber, B. A., Zambianchi, E., and Visbeck, M., 2009. Western Ross Sea continental slope gravity currents, Deep-Sea Res. Pt. II, 56, 796–817. doi: 10.1016/j.dsr2.2008.10.037

Hagen, S., Hald, M., 2002. Variation in surface and deep water circulation in the Denmark Strait, North Atlantic, during marine isotope stages 3 and 2. Paleoceanography 17, 13-1 to 13-16 (doi:10.1029/2001PA000632).

Hammer, O., Harper, D.A.T., Ryan, P.D., 2001. PAST: paleontological statistics software package for education and data analysis. Palaeontologia Electronica, 4.1.4A, 1-9 http://palaeo-electronica.org/2001_1/past/issue1_01.htm

Hansen, B., Østerhus, S., 2000. North Atlantic-Nordic Seas exchanges. Progress In Oceanography 45, 109-208.

Hemming, S.R., 2004. Heinrich Events: Massive late Pleistocene detritus layers of the North Atlantic and their global climate imprint. Reviews of Geophysics 42, RG1005/2004.

Higgins, A.K., Gilotti, J.A., Smith, P.M., 2008. The Greenland Caledonides. Evolution of the northeast margin of Laurentia. Geological Society of America, Boulder, CO, p. 368.

Hillaire-Marcel, C., de Vernal, A., Bilodeau, G., Weaver, A.J., 2001. Absence of deep-water formation in the Labrador Sea during the last interglacial period. Nature 410, 1073-6.

Howe, J.N.W., Piotrowski, A.M., Noble, T.L., Mulitza, S., Chiessi, C.M., Bayon, G., 2016. North Atlantic Deep Water production during the Last Glacial Maximum. Nature Communications 7, 11765. doi: 10.1038/ncomms11765

Hughes, A.L.C., Gyllencreutz, R., Lohne, O.S., Mangerud, J., Svendsen, J.I., 2016. The last Eurasian ice sheets - a chronological database and time-slice reconstruction, DATED-1. Boreas 45, 1-45.

Jacobs, S.S., 2004. Bottom water production and its links with the thermohaline circulation. Antarctic Science 16, 427–437.

Jennings, A.E., Hald, M., Smith, L.M., Andrews, J.T., 2006. Freshwater forcing from the Greenland Ice Sheet during the Younger Dryas: Evidence from southeastern Greenland shelf cores. Quaternary Science Reviews 25, 282-298.

Jiang, H., Eiriksson, J., Schulz, M., Knudsen, K.-L., Seidenkrantz, M.-S., 2005. Evidence for solar forcing of sea-surface temperature on the North Icelandic Shelf during the late Holocene. Geology 33, 73-76.

Jonkers, L., Moros, M., Prins, M.A., Dokken, T., Dahl, C.A., Dijkstra, N., Perner, K., Brummer, G.J.A., 2010. A reconstruction of sea surface warming in the northern North Atlantic during MIS 3 ice-rafting events. Quaternary Science Reviews. 29, 1791–1800.

Jonkers, L., Prins, M.A., Moros, M., Weltje, G.J., Troelstra, S.R., Brummer, G.J.A., 2012. Temporal offsets between surface temperature, ice-rafting and bottom flow speed proxies in the glacial (MIS 3) northern North Atlantic. Quaternary Science Reviews. 48, 43–53.

Jonsson, S., Valdimarsson, H., 2004. A new path for the Denmark Strait overflow water from the Iceland Sea to Denmark Strait. Geophysical Research Letters 31, 012004. 4pp. doi:10.1029/2003GL019214,

Kabacoff, R.I., 2015. R in Action. Data analysis and graphics with R, 2nd ed. Manning, Shelter Island, NY.

Keigwin, L.D., Swift, S.A., 2017. Carbon isotope evidence for a northern source of deep water in the glacial western North Atlantic. Proceedings of the National Academy of Sciences of the United States of America 114, 2831-2835.

Kleiven, H.F., Hall, I.R., McCave, I.N., Knorr, G., Jansen, E., 2011. Coupled deep-water flow and climate variability in the Mid-Pleistocene North Atlantic. Geology 39, 343-346

Kolla, V., Biscaye, P.E., Hanley, A.F., 1979. Distribution of quartz in Late Quaternary sediments in relation to climate. Quaternary Research 11, 261-277.

Koseoglu, D., Belt, S.T., Smik, L., Yao, H.Y., Panieri, G., Knies, J., 2018. Complementary biomarker-based methods for characterising Arctic sea ice conditions: A case study comparison between multivariate analysis and the PIP_{25} index. Geochimica et Cosmochimica Acta 222, 406-420.

Kosters, F., Kase, R., Flemming, K., Wolf, D., 2004. Denmark Strait overflow for Last Glacial Maximum to Holocene conditions. Paleoceanography 19, p. 1 to 11, PA2019.

Krumbein, W.C., Dacey, M.F., 1969. Markov chains and embedded Markov chains in geology. Mathematical Geology 1, 79-96.

Kuijpers, A., Troelstra, S.R., Prins, M.A., Linthout, K., Akhmetzhanov, A., Bouryak, S., Bachmann, M.F., Lassen, S., Rasmussen, S., Jensen, J.B., 2003. Late Quaternary sedimentary processes and ocean circulation changes at the Southeast Greenland margin. Marine Geology 195, 109-129.

Labeyrie, L., Jansen, E., Cortijo, E., 2003. Les rapports de campagnes a la mer MD114/IMAGES V. Institut Polaire Francais Paul-Emile Victor, Brest.

Labeyrie, L.D., Jennings, A.E., 2005. Physical properties of sediment core MD99-2323. https://doi.org/10.1594/PANGAEA.256517

Larsen, B., 1983. Geology of the Greenland-Iceland Ridge in the Denmark Strait, in: Bott, M.H.P., Saxov, S., Talwani, M., Thiede, J. (Eds.), Structure and Development of the Greenland-Scotland Ridge. Plenum Publishing Corp., London, pp. 425-444.

Lisiecki, L.E., Raymo, M.E., 2005. A Pliocene-Pleistocene stack of 57 globally distributed benthic $\delta^{18}O$ records. Paleoceanography 20, 17pp., PA1003, doi: 10.1029.2004PA001071

MacAyeal, D.R., 1993. Binge/purge oscillations of the Laurentide Ice Sheet as a cause of North Atlantic's Heinrich events. Paleoceanography 8, 775-784.

Marienfeld, P., 1992. Recent sedimentary processes in Scoresby Sund, East Greenland. Boreas 21, 169-186.

Masse, G., Rowland, S.J., Sicre, M.-A., Jacob, J., Belt, S.T., 2008. Abrupt climate changes for Iceland during the last millenium: Evidence from high resolution sea ice reconstructions. Earth and Planetary Science Letters, 1 of 5. doi.10.1016/j.epsl.2008.

Mao, L., Piper, D.J.W., Saint-Ange, F., Andrews, J.T., 2018. Labrador Current fluctuation during the last glacial cycle. Marine Geology 395, 234-246.

Marienfeld, P., 1992. Recent sedimentary processes in Scoresby Sund, East Greenland. Boreas 21, 169-186.

Mazaud, A., 2005. User-friendly software for vector analysis of the magnetiztion of long sediment cores. Gechemistry, Geophysics, Geosystems 6, Q12006, doi:12010.11029/12005GC001036.

McCartney, M.S., 1992. Recirculating components to the deep boundary current of the northern North Atlantic. Progress In Oceanography, 29, 283-383.

McCave, I.N., Andrews, J.T., 2019a. Distinguishing current effects in sediments delivered to the ocean by ice. I. Principles, methods and examples. Quaternary Science Reviews. 212, 92-107.

McCave, I.N., Andrews, J.T., 2019b. Distinguishing current effects in sediments delivered to the ocean by ice. II. Glacial to Holocene changes in high latitude North Atlantic upper ocean flows. Quaternary Science Reviews. 223, No. 105902.

McCave, I.N., Manighetti, B., Robinson, S.G., 1995. Sortable silt and fine sediment size/composition slicing: Parameters for palaeocurrent speed and palaeoceanography. Paleoceanography 10, 593-610.

McCave, I.N., Thornalley, D.J.R., Hall, I.R., 2017. Relation of sortable silt grain-size to deep-sea current speeds: Calibration of the 'Mud Current Meter'. Deep-Sea Research Part I, 127, 1-12.

McCave, I.N., Tucholke, B.E., 1986. Deep current-controlled sedimentation in the western North Atlantic, in: Vogt, P.R., Tucholke, B.E. (Eds.), The Geology of North America: The Western North Atlantic Region. Geological Society of America, Boulder,CO, pp. 451-468.

Mienert, J., Andrews, J.T., Milliman, J.D., 1992. The East Greenland Continental Margin (65 N) since the last deglaciation: Changes in sea floor properties and ocean circulation. Marine Geology 106, 217-238.

Miesch, A.T., 1976. Q-Mode factor analysis of compositional data. Comput. Geosci. 1,147–159.

Miller, G.H., 2008. Greenland's elusive Younger Dryas. Quaternary Science Reviews 27, 2271-2272.

Miller, R.L., Kahn, J.S., 1962. Statistical analysis in the Geological Sciences. John Wiley and Sons, Inc., New York.

Moles, J.D., McGarvie, D., Stevenson, J.A., Sherlock, S.C., Abbott, P.M., Jenner, F.E., Halton, A.M., 2019. Widespread tephra dispersal and ignimbrite emplacement from a subglacial volcano (Torfajokull, Iceland). Geology 47, 577-580.

Müller-Michaelis, A., Uenzelmann-Neben, G., 2014. Development of the Western Boundary Undercurrent at Eirik Drift related to changing climate since the early Miocene. Deep-Sea Research I 93, 21-34.

Nam, S.-I., Stein, R., Grobe, H., Hubberten, H., 1995. Late Quaternary glacial/interglacial changes in sediment composition at the East Greenland continental margin and their paleoceanographic implications. Marine Geology 122, 243-262.

Nam, S.I., Stein, R., 1999. Late Quaternary variations in sediment accumulation rates and their paleoenvironment implications: a case study from the East Greenland continental margin. GeoResearch Forum 5, 223-240.

Ogilvie, A.E.J., Jonsdottir, I., 2000. Sea ice, climate, amd Icelandic fisheries in the eighteenth and nineteenth centuries. Arctic 53, 383-394.

Ogilvie, A.E.J., Jonsson, T., 2001. The iceberg in the mist: northern research in pursuit of a “Little Ice Age”. Kluwer Academic Press., Boston, p. 263.

Paillard, D., Labeyrie, L., Yiou, P., 1996. Macintosh program performs time-series analysis. EOS 77, 379.

Parnell-Turner, R., White, N.J., McCave, I.N., Henstock, T.J., Murton, B., Jones, S.M., 2015. Architecture of North Atlantic contourite drifts modified by transient circulation of the Icelandic mantle plume, Geochemistry Geophysics, Geosystems 16, 3414–3435, doi:10.1002/2015GC005947.

Patton, H., Hubbard, A., Bradwell, T., Schomacker, A., 2017. The configuration, sensitivity and rapid retreat of the Late Weischelian Icelandic Ice Sheet. Earth-Science Reviews 166, 223-245.

Petersen, S.V., Schrag, D.P., Clark, P.U., 2013. A new mechanism for Dansgaard-Oeschger cycles. Paleoceanography 28, 24-30.

Prins, M.A., Bouwer, L.M., Beets, C.J., Troelstra, S.R., Weltje, G.J., Kruk, R.W., Kruijpers, A., Vroon, P.Z., 2002. Ocean circulation and iceberg discharge in the glacial North Atlantic: Inferences from unmixing of sediment sizes. Geology 30, 555-558.

Poore, R. Z., Osterman, L., Curry, W. B., Phillips, R. L., 1999. Late Pleistocene and Holocene meltwater events in the western Arctic Ocean. Geology 27(8), 759-762.

Prokoph, A., El Biali, H., 2008. Cross-Wavelet Analysis: A tool for detection of relationships between paleoclimate proxy records. Mathematical Geosciences, 40, 576-586. DOI 10.1007/s11004-008-9170-8

Rasmussen, S.O., Bigler, M., Blockley, S.P., Blunier, T., Buchardt, S.L., Clausen, H.B., Cvijanovic, I., Dahl-Jensen, D., Johnsen, S.J., Fischer, H., Gkinis, V., Guillevic, M., Hoek, W.Z., Lowe, J.J., Pedro, J.B., Popp, T., Seierstad, I.K., Steffensen, J.P., Svensson, A.M., Vallelonga, P., Vinther, B.M., Walker, M.J.C., Wheatley, J.J., Winstrup, M., 2014. A stratigraphic framework for abrupt climatic changes during the Last Glacial period based on three synchronized Greenland ice-core records: refining and extending the INTIMATE event stratigraphy. Quaternary Science Reviews 106, 14-28.

Rebesco, M., Hernandez-Molina, F.J., Van Rooij, D., Wahlin, A., 2014. Contourites and associated sediments controlled by deep-water circulation processes: State-of-the-art and future considerations. Marine Geology 352, 111-154.

Reeh, N., Mayer, C., Miller, H., Thomsen, H.H., Weidick, A., 1999. Present and past climate control on fjord glaciations in Greenland: Implications for IRD-deposition in the sea. Geophysical Research Letters 26, 1039-1042.

Reimann, C., Filzmoser, P., Garrett, R.G., 2002. Factor analysis applied to regional geochemical data: problems and possibilities. Applied Geochemistry 17, 185-206.

Robinson, S.G., Maslin, M.A., McCave, I.N., 1995. Magnetic susceptibility variations in upper Pleistocene deep-sea sediments of the N.E. Atlantic: Implications for ice rafting and palaeocirculation at the Last Glacial Maximum. Paleoceanography 10, 221-250.

Roesch, A and Schmidbauer, 2018a: WaveletComp: Computational Wavelet Analysis. R package 1.1. https//CRAN.R-project.org/package=Wavelet.Comp.

Roesch, A and Schmidbauer, 2018b: WaveletComp 1.1:A guided tour through the R package. 58 pp. http://www.hs-stat.com/projects/WaveletComp/WaveletComp_guided_tour.pdf

Siegel, S., 1956. Nonparametric statistics. McGraw-Hill Book Co., Inc., New York.

Skinner, L., & McCave, I. N., 2003. Analysis and modelling of the behaviour of gravity and piston corers based on soil mechanical principles. Marine Geology, 199, 181–204.

Skinner, L.C., Muschitiello, F., Scrivner, A.E., 2019. Marine reservoir age variability over the last deglaciation: Implications for marine carbon cycling and prospects for regional radiocarbon calibrations Paleoceanography and Paleoclimatology 34, 1807-1815.

Stein, A.B., 1996. Seismic stratigraphy and seafloor morphology of the Langerlussuaq region, East Greenland: Evidnece for glaciations to the Continental Shelf break during the late Weischelian Age and earlier, Geological Sciences. University of Colorado, Boulder, p. 293 pp.

Stein, R., 2008. Arctic Ocean Sediments. Processes, proxies, and Paleoenvironment. Elsevier, New York.

Stein, R., Grobe, H., Hubberten, H., Marienfeld, P., Nam, S., 1993. Latest Pleistocene to Holocene changes in glaciomarine sedimentation in Scorsby Sund and along the adjacent East Greenland Continental Margin: Preliminary results. Geo-Marine Letters 13, 9-16.

Stein, R., Nam, S.-I., Grobe, H., Hubberten, H., 1996. Late Quaternary glacial history and short-term ice-rafted debris fluctuations along the East Greenland continental margin, in: Andrews, J.T., Austen, W.A., Bergsetn, H., Jennings, A.E. (Eds.), Late Quaternary paleoceanography of North Atlantic margins. Geological Society, London, pp. 135-151.

Stein, R., Nam, S.-I., Schubert, C., Vogt, C., Fütterer, D., Heinemeier, J., 1994. The last deglaciation event in the eastern central Arctic Ocean. Science 264, 692-696.

Stern J.V., Lisiecki L.E., 2013. North Atlantic circulation and reservoir age changes over the past 41,000years. Geophysical Research Letters 40, 3693– 3697.

Stokes, C.R., Clark, C.D., Darby, D.A., Hodgson, D.A., 2005. Late Pleistocene ice export events into the Arctic Ocean from the M'Clure Strait Ice Stream, Canadian Arctic Archipelago. Global and Planetary Change 49, 139-162.

Stokes, C.R., Tarasov, L., Blomdin, R., Cronin, T.M., Fisher, T.G., Gyllencreutz, R., Hattestrand, C., Heyman, J., Hindmarsh, R.C.A., Hughes, A.L.C., Jakobsson, M., Kirchner, N., Livingstone, S.J., Margold, M., Murton, J.B., Noormets, R., Peltier, W.R., Peteet, D.M., Piper, D.J.W., Preusser, F., Renssen, H., Roberts, D.H., Roche, D.M., Saint-Ange, F., Stroeven, A.P., Teller, J.T., 2015. On the reconstruction of palaeo-ice sheets: Recent advances and future challenges. Quaternary Science Reviews 125, 15-49.

Stoner, J.S., Jennings, A.E., Kristjansdottir, G.B., Andrews, J.T., Dunhill, G., Hardardottir, J., 2007. A paleomagnetic approach toward refining Holocene radiocarbon based chronostratigraphies:

Paleoceanographic records from North Iceland (MD99-2269) and East Greenland (MD99-2322) margins. Palaeoceanography 22, 1 0f 23. PA1209, doi:1210:1029/2006PA001285, 002007.

Svensson, A., and 13 others, 2008. A 60 000 year Greenland stratigraphic ice core chronology. Climate of the Past, 4, 47–57. www.clim-past.net/4/47/2008/

Swift, J.H., 1984. The circulation of the Denmark Strait and Iceland Scotland overflow waters in the North-Atlantic. Deep-Sea Research 31, 1339-1355

Syvitski, J.P.M., Andrews, J.T., Dowdeswell, J.A., 1996. Sediment deposition in an iceberg-dominated Glacimarine Environment, East Greenland: Basin Fill Implications. Global and Planetary Change 12, 251-270.

Telford, R.J., Heegaard, E., Birks, H.J.B., 2003. All age-depth models are wrong: but how badly? Quaternary Science Reviews 23, 1-5.

Thornalley, D.J.R., McCave I.N., Elderfield H., 2011.Tephra in deglacial ocean sediments south of Iceland: Stratigraphy, geochemistry and oceanic reservoir ages**.** Journal of Quaternary Science*,* 26, 190-198.

Trachsel, M., Telford, R.J., 2017 All age-depth models are wrong, but are getting better. Holocene 27, 860-869.

Uenzelmann-Neben, G., Gruetzner, J., 2018. Chronology of Greenland Scotland Ridge overflow: What do we really know? Marine Geology 406, 109-118.

van Kreveld, S., Sarthein, M., Erlenkeuser, H., Grootes, P., Jung, S., Nadeau, M.J., Pflaumann, U., Voelker, A., 2000. Potential links between surging ice sheets, circulation changes, and the Dansgaard-Oeschger cycles in the Irminger Sea, 60-18 ka. Paleoceanography 15, 425-442.

Vasskog, K., Langebroek, P.M., Andrews, J.T., Nilsen, J.E.O., Nesje, A., 2015. The Greenland Ice Sheet during the last glacial cycle: Current ice loss and contribution to sea-level rise from a palaeoclimatic perspective. Earth-Science Reviews 150, 45-67.

Vermeesch, P., 2006. Tectonic discrimination of basalts with classification trees. Geochimica Et Cosmochimica Acta 70, 1839-1848.

Visbeck, M. & Thurnherr, A. M., 2009. High-resolution velocity and hydrographic observations of the Drygalski Trough gravity plume. Deep Sea Research, Part II, 56, 835– 842.

Voelker, A.H.L., Haflidason, H., 2015. Refining the Icelandic tephrachronology of the last glacial period - the deep-sea core P52644 record from the southern Greenland Sea. Global and Planetary Change 131, 35–62.

Voelker, A.H.L., 1999. Zur Deutung der Dansgaard-Oeschger Ereignisse in ulta-hochauflosenden Sedimentprofilen aus dem Europaischen Nordmeer, Dansgaard-Oeschger events in ultra-high resolution sediment records from the Nordic Seas. Universitat Kiel, Kiel, p. 271.

Voelker, A.H.L., 2002, Global distribution of centennial-scale records for Marine Isotope Stage (MIS) 3: a database. Quaternary Science Reviews 21,1185-1212, doi: 10.1016/S0277-3791(01)00139-1

Vogt, C., 1997. Regional and temporal variations of mineral assemblages in Arctic Ocean sediments as climatic indicators during Glacial/Interglacial changes. Reports on Polar Research 251, 1-309.

Vogt, C., Knies, J., 2008. Sediment dynamics in the Eurasian Arctic Ocean during the last deglaciation--The clay mineral group smectite perspective. Marine Geology 250, 211-222.

von Appen, W.J., Mastropole, D., Pickart, R.S., Valdimarsson, H., Jonsson, S., Girton, J.B., 2017. On the nature of the mesoscale variability in Denmark Strait. Journal of Physical Oceanography 47, 567-582.

Yoon, S.T., Lee, W.S., Stevens, C., Jendersie, S., Nam, S., Yun, S., Hwang, C.Y., Jang, G.I., Lee, J., 2020. Variability in high-salinity shelf water production in the Terra Nova Bay polynya, Antarctica. Ocean Science 16, 373–388. doi: 10.5194/os-16-373-2020

Highlights

- 240 cal ka record of changes in current speed and grain-size
- Snorri Drift----Northern-most Atlantic sediment drift
- Changes in mineral composition indicate changes in sediment sources
- Grain-size and mineral records implicate links to orbital forcing
- MD99-2323 within 130 km of the limits of the Iceland and Greenland ice sheets